

Gradient Boosted Mixed Models: Flexible Joint Estimation of Mean and Variance Components for Clustered Data

Mitchell L. Prevett*, Francis K. C. Hui, Zhi Yang Tho, A. H. Welsh, Anton H. Westveld

Research School of Finance, Actuarial Studies and Statistics,
The Australian National University, Canberra, ACT 2601, Australia

October 31, 2025

Abstract

Linear mixed models are widely used for clustered data, but their reliance on parametric forms limits flexibility in complex and high-dimensional settings. In contrast, gradient boosting methods achieve high predictive accuracy through nonparametric estimation, but do not accommodate clustered data structures or provide uncertainty quantification.

We introduce Gradient Boosted Mixed Models (GBMixed), a framework and algorithm that extends boosting to jointly estimate mean and variance components via likelihood-based gradients. In addition to nonparametric mean estimation, the method models both random effects and residual variances as potentially covariate-dependent functions using flexible base learners such as regression trees or splines, enabling nonparametric estimation while maintaining interpretability.

Simulations and real-world applications demonstrate accurate recovery of variance components, calibrated prediction intervals, and improved predictive accuracy relative to standard linear mixed models and nonparametric methods. GBMixed provides heteroscedastic uncertainty quantification and introduces boosting for heterogeneous random effects. This enables covariate-dependent shrinkage for cluster-specific predictions to adapt between population and cluster-level data. Under standard causal assumptions, the framework enables estimation of heterogeneous treatment effects with reliable uncertainty quantification.

Keywords: Gradient boosting; Mixed-effects models; Distributional learning; Covariate-dependent random effects; Uncertainty quantification; Treatment effect heterogeneity.

*Corresponding author: mitchell.prevett@anu.edu.au

1 Introduction

Mixed models are widely recognized as a fundamental tool for statistical inference, particularly in applications involving clustered (grouped) data. By including random effects, they capture within-cluster correlation and separate variability into components, enabling inference on both population and cluster level effects.

Linear mixed models are widely used in experimental and observational studies. However, their reliance on predefined functional forms can limit their flexibility, particularly when applied to complex, high-dimensional data where predictive accuracy is a primary concern. In contrast, gradient boosting has emerged as one of the most powerful predictive modeling techniques in machine learning, constructing highly flexible, nonparametric models that excel in capturing nonlinear relationships and complex interactions. Despite its strong predictive performance, gradient boosting assumes independent observations and lacks capacity to model clustered or correlated data. Also, it does not provide variance decomposition or prediction intervals without additional modifications.

To address this gap, we introduce **Gradient Boosted Mixed Models (GBMixed)**, an algorithm that integrates gradient boosting with mixed-effects modeling. We extend boosting to clustered data, enabling flexible, data-driven estimation while retaining the capacity for statistical inference. We do so by (i) generalizing boosting beyond mean functions to model random effects and residual variance components, (ii) allowing modular base learners for each component (ranging from constant updates to heteroscedastic, covariate-dependent variance models), and (iii) formulating updates through likelihood-based gradients, which provide joint estimation of mean and variance via pseudo-responses. Through simulation studies and real-world applications, we demonstrate that GBMixed delivers improved predictive performance, accurate recovery of variance components, and calibrated intervals relative to standard linear mixed models and nonparametric methods.

These contributions establish GBMixed as a general framework that combines the predictive strength of gradient boosting with the variance decomposition of linear mixed models. It encompasses both linear mixed effects models and gradient boosting machines as special cases, providing familiar reference points. The framework further extends to nonparametric mixed effects models through four variants that introduce covariate-dependent modeling of both residual and random-effects variances, the latter representing the first known boosting based approach to heterogeneous random effects. By allowing random-effects to vary with covariates, GBMixed induces covariate-dependent shrinkage, whereby the degree of pooling between group and population predictions adapts to observed features. This framework enables improved mean and variance estimation providing broad applicability to predictive modeling in clustered data settings.

We organize the remainder of the paper as follows. Section 2 provides background and an overview of related work. Section 3 introduces the GBMixed model, baseline form and heterogeneous variance

form. Section 4 describes the boosting algorithm, including initialization, gradient computation, base learner modeling and iterative updates for mean and variance components. Section 5 presents simulation experiments evaluating predictive performance, variance estimation, and inference for heterogeneous treatment effects. Section 6 presents real-world case studies on the Primary Biliary Cirrhosis (PBC) data from the Mayo clinic and the Panel Study of Income Dynamics (PSID) from the long-running U.S. household survey. Section 7 concludes with a discussion, limitations, and directions for future work. Additional implementation details, simulation diagnostics, and supplementary results are provided in the appendices.

2 Background and Related Work

2.1 Gradient Boosting

Introduced as a functional gradient descent view of boosting by Mason et al. (1999) and Friedman (2001), gradient boosting machines (GBMs) have established themselves as one of the most influential ensemble methods for modern regression and classification. GBMs are particularly effective at capturing complex, nonlinear relationships and interactions in high-dimensional data while maintaining strong generalization properties. The choice of loss function, base learner complexity, subsampling, and tree constraints all play crucial roles in its performance along with preventing overfitting. While particularly strong in predictive accuracy, standard implementations of GBMs are primarily designed for point estimation and lack formal statistical inference, limiting their use in applications requiring reliable uncertainty quantification or modeling of clustered data structures.

2.2 Mixed Effects Models

Linear mixed models (LMMs; Henderson, 1950) represent a key generalization of classical regression, designed to account for correlation among observations, for example within clustered or hierarchical data structures.

Building on the classical linear case, nonlinear mixed models (Lindstrom and Bates, 1990) allow fixed effects to vary nonlinearly, thereby broadening applicability in settings where linear assumptions are inadequate. Later developments (Ruckstuhl et al., 2000; Karcher and Wang, 2001; Gu and Ma, 2005) incorporated nonparametric estimation of fixed effects, delivering hybrid models that combine flexible covariate functions with linear random effects. These approaches have been valuable for longitudinal analyses, though reliance on spline bases has limitations for extrapolation in prediction and there is little attention on modeling variance components.

2.3 Modern Nonparametric and Distributional Methods

Recent work in nonparametric and distributional methods has aimed to move beyond point estimation toward flexible modeling of heterogeneous effects and full predictive distributions.

Causal forests (Wager and Athey, 2017) extend the random forest (Breiman, 2001) framework to estimate heterogeneous treatment effects (HTEs) and provide statistical inference. By targeting the Conditional Average Treatment Effect (CATE), causal forests capture how treatment effects vary across individuals or subgroups in a data-driven manner, along with estimation of measures of uncertainty. That said, they do not explicitly incorporate random effects or clustered data structures, which limits their applicability in these settings.

Natural Gradient Boosting (NGBoost; Duan et al., 2019), extends traditional gradient boosting by shifting the focus from predicting single-point estimates to modeling the entire probability distribution of the response variable. Unlike standard gradient boosting methods, which optimize for a specific loss function to produce point predictions, NGBoost estimates conditional probability distributions by parameterizing the likelihood function. This approach enables the model to quantify uncertainty in predictions, providing not only expected values but also variance and higher-order moments.

A related parametric approach is Generalized Additive Models for Location, Scale, and Shape (GAMLSS; Rigby and Stasinopoulos, 2005), which allows all parameters of the response distribution (such as the mean, variance, skewness, and kurtosis) to depend on covariates through additive predictors. While GAMLSS models provide rich probabilistic structure and flexibility in distributional assumptions, they typically rely on generalized additive model (GAM) components and lack scalability in high-dimensional or non-linear settings. Like NGBoost, classical GAMLSS implementations also assume independent observations and do not account for clustered structures.

Another related direction is double machine learning (DML; Chernozhukov et al., 2018), which provides a technique for estimating causal parameters in high-dimensional settings using machine learning methods for nuisance functions. These nuisance functions represent high-dimensional relationships (such as outcome regressions or propensity scores) that are not themselves of interest but must be estimated to infer or remove bias from the target causal parameter. DML leverages sample-splitting and orthogonalization to enable inference under weaker assumptions than classical regression, and has been extended to allow for clustered standard errors and panel data structures. Nonetheless, DML does not explicitly model random effects variance components or the full covariance structure of clustered data models.

These approaches collectively demonstrate the progress made in moving machine learning beyond black-box prediction toward causal and distributional inference. Yet, to our knowledge, none jointly combine nonparametric mean estimation with variance component modeling for clustered data.

2.4 Nonparametric Bayesian Structured Models

Bayesian methods have also been extended to incorporate clustered structure within nonparametric models. One example is the random-intercept Bayesian Additive Regression Trees (riBART; Tan and Roy, 2019). Standard BART assumes independent observations, which can be restrictive in clustered settings. riBART extends this framework by incorporating random intercepts to account for within-cluster correlation, such as repeated measures from the same subject. This modification improves predictive accuracy in clustered data while preserving BART’s nonparametric flexibility. That said, riBART is limited to random intercept structures and requires fully Bayesian estimation, which can be computationally expensive compared to boosting-based approaches.

Another line of work is the Bayesian Deep Net GLM and GLMM (Tran et al., 2019), which integrates deep neural networks with generalized linear models (GLMs) and generalized linear mixed models (GLMMs). In this algorithm, the neural network captures complex nonlinearities in the fixed effects while the Bayesian formulation provides uncertainty quantification and interpretability. Empirical results on both simulated and real datasets demonstrate superior predictive accuracy and uncertainty calibration compared to traditional GLMs, GLMMs, and standard deep learning models. Nonetheless, these methods are constrained by their reliance on a single model class (deep feedforward neural networks for the mean structure) which limits their flexibility for different modeling tasks. They are not explicitly designed for heterogeneous treatment effect estimation, and share well-known challenges of deep learning such as high computational cost, long training times, and sensitivity to hyperparameter choices.

These approaches illustrate the potential of combining clustered data modeling with nonparametric and deep learning techniques. That said, they remain restricted in scope, either limited to simple random intercept structures or tied to computationally intensive Bayesian and neural network architectures.

2.5 Boosting within Structured Random Effects

Several recent approaches have combined boosting with structured or clustered data models. The MERMBoost algorithm, (Kniper et al., 2025), extends the `mboost` package (Bühlmann and Hothorn, 2007) to fit mixed-effects generalized additive models using gradient boosting. In this approach, boosting iterations update nonparametric smooth components for selected predictors while simultaneously optimizing random effect terms. An adjustment is included to reduce bias in the estimation of random effects, a limitation observed in earlier boosting approaches to mixed models. MERMBoost demonstrates strong predictive performance across several benchmark experiments and supports a range of random effect structures. However, its focus on additive models, where each predictor is fit independently at each boosting step, constrains its ability to capture higher-order interactions compared to other boosting methods.

A related line of work is Gaussian Process Boosting (GPBoost), (Sigrist, 2022). GPBoost integrates

tree boosting with Gaussian processes, enabling nonparametric modeling of the mean function while explicitly accounting for grouped random effects and spatial correlation. The algorithm alternates between boosting the mean component and optimizing Gaussian process covariance parameters conditional on the boosted estimates. This design provides flexibility in modeling nonlinear mean structures and complex correlation patterns. However, similar to MERMBoost, it can suffer from bias in random effect estimation due to the sequential treatment of mean and variance components (incrementally boosted for mean and fully optimized for the variance components). Moreover, GPBoost inherits the computational challenges of Gaussian process models, which may limit scalability in high-dimensional or large-sample settings.

These methods highlight the promise of combining boosting with structured modeling of random effects while also outlining the current limitations.

3 Model

We now introduce Gradient Boosted Mixed Models (GBMixed), a framework that extends mixed-effects modeling through gradient-based boosting of both mean and variance components. We begin by presenting the baseline form of the model, which extends the classical linear mixed model to incorporate nonparametric estimation of both the mean function and variance components. This section introduces the observation-level formulation, the associated variance decomposition, and a generalization to covariate-dependent variance structures. Estimation procedures are described in Section 4.

3.1 Baseline Model

We consider a standard linear mixed model augmented with a nonparametric representation of the mean function. At the observation level, the model is written as

$$y_{ij} = f(\mathbf{x}_{ij}) + \mathbf{z}_{ij}^\top \mathbf{u}_i + \varepsilon_{ij}, \quad i = 1, \dots, C, \quad j = 1, \dots, n_i. \quad (3.1)$$

Let $n = \sum_{i=1}^C n_i$ denote the total number of observations across all groups. The quantities $y_{ij}, \mathbf{x}_{ij}, \mathbf{z}_{ij}$ are observed, while \mathbf{u}_i and ε_{ij} are latent. y_{ij} denotes the response for observation j in group i , \mathbf{x}_{ij} is the vector of p covariates, and $f(\cdot)$ is a generic, possibly nonlinear and complex function that may include multilevel interactions, representing the relationship between the covariates and the response. The mean component (population-level expectation or marginal mean) is $\mu_{ij} = f(\mathbf{x}_{ij}) = \mathbb{E}[Y_{ij} \mid \mathbf{x}_{ij}]$, representing the expected response for a given covariate profile. The term $\mathbf{z}_{ij}^\top \mathbf{u}_i$ captures group-specific random effects, where \mathbf{z}_{ij} is the random effects design vector of dimension q . Also $\mathbf{u}_i \stackrel{\text{i.i.d.}}{\sim} N(\mathbf{0}, \mathbf{G})$ is the group-level random effects vector, with $\mathbf{u}_i \in \mathbb{R}^q$ and covariance matrix $\mathbf{G} \in \mathbb{R}^{q \times q}$. Residual variation is modeled by

$$\varepsilon_{ij} \stackrel{\text{i.i.d.}}{\sim} N(0, \sigma^2),$$

with constant residual variance σ^2 across all observations.

Marginalizing this model over the random effects yields the distribution of the response vector for group i as

$$\mathbf{y}_i \sim N(\boldsymbol{\mu}_i, \boldsymbol{\Sigma}_i), \quad (3.2)$$

where $\mathbf{y}_i = (y_{i1}, \dots, y_{in_i})^\top \in \mathbb{R}^{n_i}$, $\boldsymbol{\mu}_i \in \mathbb{R}^{n_i}$ is the mean component, and $\boldsymbol{\Sigma}_i \in \mathbb{R}^{n_i \times n_i}$ is the marginal covariance matrix of \mathbf{y}_i . The variance decomposition for $\boldsymbol{\Sigma}_i$ is detailed in Section 3.2. The mean vector is given by

$$\boldsymbol{\mu}_i = f(\mathbf{X}_i) = \begin{bmatrix} f(\mathbf{x}_{i1}) \\ f(\mathbf{x}_{i2}) \\ \vdots \\ f(\mathbf{x}_{in_i}) \end{bmatrix},$$

where $\mathbf{X}_i \in \mathbb{R}^{n_i \times p}$ is the design matrix of covariates for group i .

3.2 Variance Decomposition

A key component of likelihood-based estimation is the marginal variance–covariance structure of the response vector, which accounts for both random effects and residual error. Under the homogeneous specification, the marginal variance of a single observation, j in group i is

$$\text{Var}(y_{ij}) = \mathbf{z}_{ij}^\top \mathbf{G} \mathbf{z}_{ij} + \sigma^2. \quad (3.3)$$

This is a scalar quantity reflecting the total variance for observation j in group i , with constant residual variance σ^2 .

At the group level, the corresponding marginal variance–covariance matrix for the response vector \mathbf{y}_i is

$$\boldsymbol{\Sigma}_i = \mathbf{Z}_i \mathbf{G} \mathbf{Z}_i^\top + \sigma^2 \mathbf{I}_{n_i}, \quad (3.4)$$

where $\mathbf{Z}_i \in \mathbb{R}^{n_i \times q}$ is the random effects design matrix for group i constructed by stacking the row vectors \mathbf{z}_{ij}^\top for all observations in the group, $\mathbf{G} \in \mathbb{R}^{q \times q}$ is the covariance matrix of the random effects, and $\sigma^2 \mathbf{I}_{n_i}$ represents the residual variance component with the identity matrix $\mathbf{I}_{n_i} \in \mathbb{R}^{n_i \times n_i}$.

While the population-level version of this model can be expressed by stacking all the groups in a single block-diagonal covariance structure, this form is not required for estimation, prediction or inference. The

group level representation provides all the quantities needed for likelihood computation and gradient boosting.

Across both forms, the matrix \mathbf{G} allows for complex dependency structures, including nested or crossed effects though the current implementation is for clustered data only. The residual variance σ^2 captures variation at the observation level and is often presented as $\mathbf{R}_i = \sigma^2 \mathbf{I}_{n_i} \in \mathbb{R}^{n_i \times n_i}$ giving this decomposition the name " \mathbf{G} and \mathbf{R} variance decomposition".

Although one could estimate Σ_i directly, the \mathbf{G} and \mathbf{R} decomposition improves interpretability, reduces computational overhead and typically leads to greater numerical stability in estimation.

3.3 Heterogeneous Variance Model Form

In many real-world applications, we observe non-constant variance either across subgroups of the population or systematically. This heteroscedasticity can be observed in either of the variance components, \mathbf{G} or \mathbf{R} and can reasonably be assumed to depend on some unknown function of the covariates. For example, the data may have been collected from two or more distinct subpopulations each with their own \mathbf{G} and \mathbf{R} matrices. To capture this heterogeneity we introduce a more general model form. Specifically, we replace the constant matrices \mathbf{G} and \mathbf{R} with matrices that vary as a function of covariates:

$$\mathbf{u}_i \sim N(\mathbf{0}, \mathbf{G}(\tilde{\mathbf{x}}_i)), \quad (3.5a)$$

$$\varepsilon_{ij} \sim N(0, R(\mathbf{x}_{ij})). \quad (3.5b)$$

Note that the output of $R(\cdot)$ depends on the dimensions of the modeled residuals. It returns a scalar when modeling individual residuals and a diagonal matrix when modeling the full residual vector.

Here, we introduce $\tilde{\mathbf{x}}_i \in \mathbb{R}^r$, a vector of group-level covariates. In order to model the heterogeneous group level random effects covariances, we need to summarize the information from the observation level covariates into a single set for the group. These group-level covariates can include: (i) those that are inherently constant at the group level (e.g., geographic region); and (ii) summary statistics derived from the observation-level covariates within cluster i , such as mean values for continuous variables or mode values for categorical variables. This construction enables $\mathbf{G}(\tilde{\mathbf{x}}_i) \in \mathbb{R}^{q \times q}$ to capture variation in the random effects covariance matrix across groups.

Using this form, the marginal variance for observation j in group i is

$$\text{Var}(y_{ij}) = \mathbf{z}_{ij}^\top \mathbf{G}(\tilde{\mathbf{x}}_i) \mathbf{z}_{ij} + R(\mathbf{x}_{ij}), \quad (3.6)$$

where $\mathbf{z}_{ij} \in \mathbb{R}^q$ is the random effects design vector, $\mathbf{G}_i = \mathbf{G}(\tilde{\mathbf{x}}_i) \in \mathbb{R}^{q \times q}$ is the random effects covariance matrix determined by group-level covariates, and $R(\mathbf{x}_{ij}) = R_{ij} \in \mathbb{R}$ is the scalar residual variance

determined by observation-level covariates.

At the group level, the marginal variance-covariance matrix for the response vector $\mathbf{y}_i \in \mathbb{R}^{n_i}$ is

$$\Sigma_i = \mathbf{Z}_i \mathbf{G}(\tilde{\mathbf{x}}_i) \mathbf{Z}_i^\top + \mathbf{R}(\mathbf{X}_i), \quad (3.7)$$

where $\mathbf{Z}_i \in \mathbb{R}^{n_i \times q}$ is the random effects design matrix for group i , and $\mathbf{R}_i = \mathbf{R}(\mathbf{X}_i) \in \mathbb{R}^{n_i \times n_i}$ is a diagonal matrix of residual variances with entries $R_{ij}, j = 1, \dots, n_i$.

This generalization nests the homogeneous model as a special case where $\mathbf{G}(\tilde{\mathbf{x}}_i) \equiv \mathbf{G}$ and $\mathbf{R}(\mathbf{X}_i) \equiv \sigma^2 \mathbf{I}_{n_i}$ for all i .

4 Boosting Algorithm

Now we introduce the boosting algorithm which forms the basis of estimation for the model. Estimation is carried out using an iterative approach that updates both mean and variance components within a single likelihood framework. To begin with we show a high level schematic of the algorithm.

4.1 Conceptual Overview

Figure 1 illustrates the high-level estimation process.

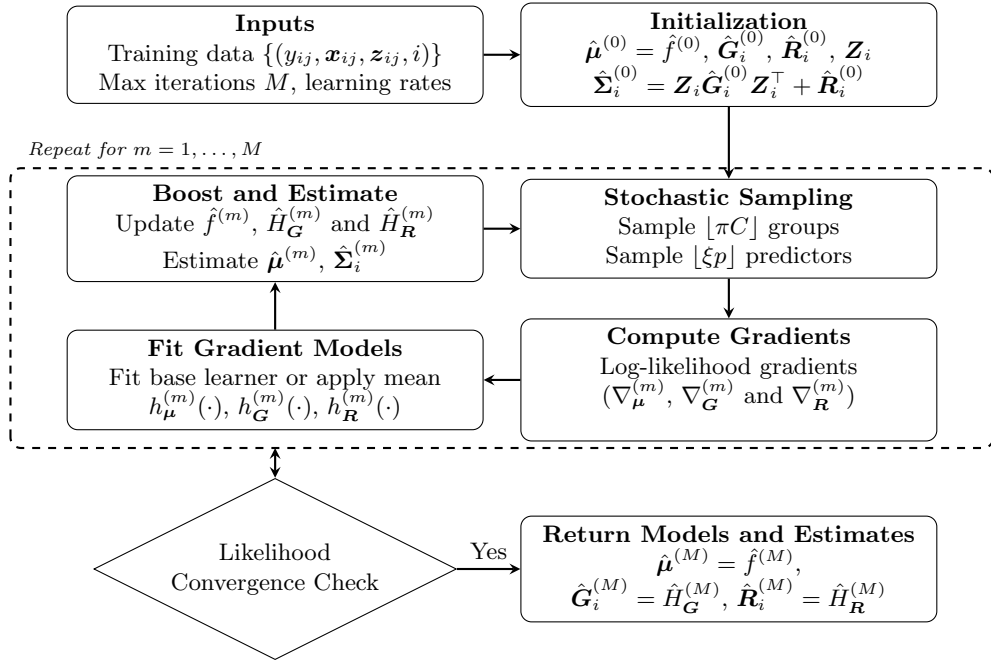


Figure 1: Flowchart of the GBMixed algorithm. At each iteration, the mean function $f(\cdot)$, random effects covariance \mathbf{G}_i , and residual variances \mathbf{R}_i are updated using gradients as pseudo-responses. Here, $\hat{\mu}$ denotes the fitted means implied by the learned function $f(\cdot)$, and $\hat{\Sigma}_i = \mathbf{Z}_i \hat{\mathbf{G}}_i \mathbf{Z}_i^\top + \hat{\mathbf{R}}_i$ is the estimated marginal covariance matrix for group i . Full definitions of the notation are provided in Section 4.2.

The algorithm alternates between stochastic sampling, computing likelihood-based gradients, fitting

base learners to those gradients, and updating the mean and variance components through additive steps. This allows flexible base learners which provide covariate-dependent estimation of both mean (fixed) and variance (random effects and residual) components. Convergence is assessed via maximization of the log-likelihood.

4.2 Algorithmic Steps

The stepwise procedure for GBMixed is outlined in Algorithm 1. This pseudocode builds on the flowchart in Figure 1, capturing the same high-level structure while detailing the individual steps and calculations at each stage.

Gradients are calculated iteratively for each group and aggregated for modeling. In some cases, transformations are applied to the gradient updates for variance components to ensure positive definiteness, as discussed further in Section 4.3. Base learners fitted at iteration m are denoted by lowercase symbols, for example $h_\mu^{(m)}$, while uppercase symbols such as $H^{(m)}$ or $f^{(m)}$ represent the accumulated ensemble prediction function. The random-effect and residual variance components can be modeled as homogeneous when $h(\cdot)$ is constant, or as covariate-dependent when $h(\cdot)$ varies with the input features. The validation or out-of-bag (OOB) dataset used to monitor convergence is written as $\mathcal{D}_{\text{eval}}$. The lookback window, k , is used for assessing convergence based on the log-likelihood for the validation data falling below the threshold δ .

Algorithm 1: Gradient Boosted Mixed Model (GBMixed)

Input: Data $\mathcal{D} = (y_{ij}, \mathbf{x}_{ij}, \mathbf{z}_{ij}, i)$; Evaluation data $\mathcal{D}_{\text{eval}} \subset \mathcal{D}$ (OOB or validation set)

Subsampling rates π and ξ ; Learning rates ν_μ, ν_G, ν_R ; max iterations M

Function classes $\mathcal{H}_\mu, \mathcal{H}_G, \mathcal{H}_R$; Base learner parameters $\theta_\mu, \theta_G, \theta_R$

Output: Models and estimates $\hat{\mu}_i^{(M)} = \hat{f}^{(M)}(\mathbf{X}_i)$, $\hat{\mathbf{G}}_i^{(M)} = \hat{H}_G^{(M)}(\tilde{\mathbf{x}}_i)$, $\hat{\mathbf{R}}_i^{(M)} = \hat{H}_R^{(M)}(\mathbf{X}_i)$

Initialize: $\hat{f}^{(0)}, \hat{H}_G^{(0)}, \hat{H}_R^{(0)}$, Grouped design matrix \mathbf{Z}_i , Group aggregated features $\tilde{\mathbf{x}}_i$

Set: $\hat{\mu}_i^{(0)} = \hat{f}^{(0)}$, $\hat{\Sigma}_i^{(0)} = \mathbf{Z}_i \hat{\mathbf{G}}_i^{(0)} \mathbf{Z}_i^\top + \hat{\mathbf{R}}_i^{(0)}$

for $m = 1$ **to** M **do**

 Draw a proportion $\pi \in (0, 1]$ of groups: $\mathcal{C}^{(m)} \subset \{1, \dots, C\}$ with $|\mathcal{C}^{(m)}| = \lfloor \pi C \rfloor$.

 Draw a proportion $\xi \in (0, 1]$ of features: $\mathcal{J}^{(m)} \subset \{1, \dots, p\}$ with $|\mathcal{J}^{(m)}| = \lfloor \xi p \rfloor$.

for $i = 1$ **to** C **do**

 Compute gradients of the log-likelihood:

$$\begin{aligned}\nabla_{\mu_i}^{(m)} &= \frac{\partial \ell}{\partial \mu_i} \Big|_{(\hat{\mu}_i^{(m-1)}, \hat{\Sigma}_i^{(m-1)})} \in \mathbb{R}^{n_i} \\ \nabla_{\mathbf{G}_i}^{(m)} &= \frac{\partial \ell}{\partial \mathbf{G}_i} \Big|_{(\hat{\mu}_i^{(m-1)}, \hat{\Sigma}_i^{(m-1)})} \in \mathbb{R}^{q \times q} \\ \nabla_{\mathbf{R}_i}^{(m)} &= \frac{\partial \ell}{\partial \mathbf{R}_i} \Big|_{(\hat{\mu}_i^{(m-1)}, \hat{\Sigma}_i^{(m-1)})} \in \mathbb{R}^{n_i}\end{aligned}$$

Fit Gradient Models - Each component is updated by fitting a base learner or constant to its respective gradient. Let $h^{(m)}$ denote the learner at iteration m . Then:

$$\begin{aligned}h_\mu^{(m)} &\leftarrow \arg \min_{h \in \mathcal{H}_\mu} \sum_{i \in \mathcal{C}^{(m)}} \left(\nabla_{\mu_i}^{(m)} - h(\mathbf{x}_{ij}, \mathcal{J}^{(m)}) \right)^2 \\ h_{\mathbf{G}}^{(m)} &\leftarrow \begin{cases} \frac{1}{|\mathcal{C}^{(m)}|} \sum_{i \in \mathcal{C}^{(m)}} \nabla_{\mathbf{G}_i}^{(m)}, & \text{if } \mathcal{H}_G = \{h : h(\cdot) = \text{const}\} \\ \arg \min_{h \in \mathcal{H}_G} \sum_{i \in \mathcal{C}^{(m)}} \left(\nabla_{\mathbf{G}_i}^{(m)} - h(\tilde{\mathbf{x}}_i, \mathcal{J}^{(m)}) \right)^2, & \text{otherwise} \end{cases} \\ h_{\mathbf{R}}^{(m)} &\leftarrow \begin{cases} \frac{1}{|\mathcal{C}^{(m)}|} \sum_{i \in \mathcal{C}^{(m)}} \nabla_{\mathbf{R}_i}^{(m)}, & \text{if } \mathcal{H}_R = \{h : h(\cdot) = \text{const}\} \\ \arg \min_{h \in \mathcal{H}_R} \sum_{i \in \mathcal{C}^{(m)}} \left(\nabla_{\mathbf{R}_i}^{(m)} - h(\mathbf{x}_{ij}, \mathcal{J}^{(m)}) \right)^2, & \text{otherwise} \end{cases}\end{aligned}$$

Boost models:

$$\hat{f}^{(m)} = \hat{f}^{(m-1)} + \nu_\mu \cdot h_\mu^{(m)}, \quad \hat{H}_G^{(m)} = \hat{H}_G^{(m-1)} + \nu_G \cdot h_{\mathbf{G}}^{(m)}, \quad \hat{H}_R^{(m)} = \hat{H}_R^{(m-1)} + \nu_R \cdot h_{\mathbf{R}}^{(m)}$$

Update estimates: $\hat{\mu}_i^{(m)} = \hat{f}^{(m)}(\mathbf{X}_i)$, $\hat{\Sigma}_i^{(m)} = \mathbf{Z}_i \hat{\mathbf{G}}_i^{(m)} \mathbf{Z}_i^\top + \hat{\mathbf{R}}_i^{(m)}$

Evaluate log-likelihood on validation data $\mathcal{D}_{\text{eval}}$: $\ell^{(m)} = \sum_{i=1}^C \log p(\mathbf{y}_{\text{eval},i} | \hat{\mu}_i^{(m)}, \hat{\Sigma}_i^{(m)})$

if $|\ell^{(m)} - \ell^{(m-k)}| < \delta$ **then**

break

return final functions: $\hat{f}^{(M)}, \hat{H}_G^{(M)}, \hat{H}_R^{(M)}$

4.3 Gradient Computation

In this section we outline the approach for computing gradients for the model, assuming a multivariate Gaussian response. Allowing for group-level heterogeneity in \mathbf{G} , and observation-level heterogeneity in \mathbf{R} , the total log-likelihood across all groups is calculated as

$$\ell(\boldsymbol{\mu}, \boldsymbol{\Sigma}) = \sum_{i=1}^C \ell_i(\boldsymbol{\mu}_i, \boldsymbol{\Sigma}_i),$$

where each group-level log-likelihood is

$$\ell_i(\boldsymbol{\mu}_i, \boldsymbol{\Sigma}_i) = -\frac{1}{2} \{ n_i \log(2\pi) + \log |\boldsymbol{\Sigma}_i| + (\mathbf{y}_i - \boldsymbol{\mu}_i)^\top \boldsymbol{\Sigma}_i^{-1} (\mathbf{y}_i - \boldsymbol{\mu}_i) \}.$$

At each boosting iteration, we compute score functions based on derivatives of the log-likelihood with respect to three components: the mean function $\boldsymbol{\mu}_i$, the random effects variance \mathbf{G}_i , and the residual variance \mathbf{R}_i . These act as pseudo-responses in the functional gradient descent scheme.

Mean gradient (per group): Differentiating the log-likelihood with respect to the mean yields the familiar score vector:

$$\nabla_{\boldsymbol{\mu}_i} = \frac{\partial \ell_i}{\partial \boldsymbol{\mu}_i} = \boldsymbol{\Sigma}_i^{-1} (\mathbf{y}_i - \boldsymbol{\mu}_i),$$

where the gradient is taken element-wise for each observation j in group i from this score vector.

Covariance gradient (per group): Differentiating with respect to the group-level covariance matrix yields the score matrix:

$$\frac{\partial \ell_i}{\partial \boldsymbol{\Sigma}_i} = -\frac{1}{2} \boldsymbol{\Sigma}_i^{-1} [\boldsymbol{\Sigma}_i - (\mathbf{y}_i - \boldsymbol{\mu}_i)(\mathbf{y}_i - \boldsymbol{\mu}_i)^\top] \boldsymbol{\Sigma}_i^{-1}.$$

Random effects variance gradient (per group): Using the decomposition $\boldsymbol{\Sigma}_i = \mathbf{Z}_i \mathbf{G}_i \mathbf{Z}_i^\top + \mathbf{R}_i$, we obtain the gradient with respect to \mathbf{G}_i via the chain rule:

$$\nabla_{\mathbf{G}_i} = \frac{\partial \ell_i}{\partial \mathbf{G}_i} = -\frac{1}{2} \left(\mathbf{Z}_i^\top \boldsymbol{\Sigma}_i^{-1} \mathbf{Z}_i - \mathbf{Z}_i^\top \boldsymbol{\Sigma}_i^{-1} (\mathbf{y}_i - \boldsymbol{\mu}_i)(\mathbf{y}_i - \boldsymbol{\mu}_i)^\top \boldsymbol{\Sigma}_i^{-1} \mathbf{Z}_i \right).$$

To ensure positive definiteness of the estimated variance components, we apply boosting with the Cholesky transformation for \mathbf{G}_i and with the log transformation for \mathbf{R}_i . Specifically, the updates for \mathbf{G}_i are applied to the entries of the Cholesky factor \mathbf{L}_i such that $\mathbf{G}_i = \mathbf{L}_i \mathbf{L}_i^\top$. The gradient is computed via the chain rule as,

$$\frac{\partial \ell}{\partial \mathbf{L}_i} = 2 \cdot \frac{\partial \ell}{\partial \mathbf{G}_i} \cdot \mathbf{L}_i,$$

which allows unconstrained optimization over the lower-triangular entries of \mathbf{L}_i while preserving the

positive semi-definiteness of \mathbf{G}_i .

Residual variance gradient (per observation): Assuming \mathbf{R}_i is diagonal, the gradient with respect to each diagonal entry is:

$$\nabla_{R_{ij}} = \frac{\partial \ell_i}{\partial R_{ij}} = -\frac{1}{2} [\Sigma_i^{-1} - \Sigma_i^{-1}(\mathbf{y}_i - \boldsymbol{\mu}_i)(\mathbf{y}_i - \boldsymbol{\mu}_i)^\top \Sigma_i^{-1}]_{jj}.$$

To ensure positive definiteness, the updates for \mathbf{R}_i are performed on $\log \mathbf{R}_i$ and applied element-wise to the diagonal entries. The derivative with respect to each log-variance is

$$\frac{\partial \ell}{\partial \log R_{ij}} = \frac{\partial \ell}{\partial R_{ij}} \cdot \frac{\partial R_{ij}}{\partial \log R_{ij}} = \frac{\partial \ell}{\partial R_{ij}} \cdot R_{ij},$$

ensuring that all variance estimates remain positive under additive updates in the transformed parameter space.

These gradients form the pseudo-responses for boosting the mean, random effect, and residual variance components. A complete derivation is provided in Appendix A; see also McCulloch and Searle, 2001, Searle et al., 2006, and Petersen and Pedersen, 2012.

4.4 Function Estimation and Base Learners

Each gradient component is modeled using a base learner, trained to minimize squared loss between the gradient pseudo-response and the base learner function. These models are fit using the pseudo-responses at each boosting step, across all subsampled groups. The approach corresponds with functional gradient ascent where each component is updated iteratively, conditional on the function estimates from the prior step.

The mean gradient $\nabla_{\mu_{ij}}^{(m)}$ and residual variance gradient $\nabla_{R_{ij}}^{(m)}$ are modeled using individual-level features \mathbf{x}_{ij} . The random effects variance gradient $\nabla_{\mathbf{G}_i}^{(m)}$, or its Cholesky-transformed form $\nabla_{\mathbf{L}_i}^{(m)}$, has only the lower-triangular elements extracted and is modeled using group-level features $\tilde{\mathbf{x}}_i$. Let $h_{\boldsymbol{\mu}}^{(m)}, h_{\mathbf{G}}^{(m)}, h_{\mathbf{R}}^{(m)}$ denote the corresponding functions (base learners) fit at iteration m . These are added to the model ensemble as additive updates. The resulting functions are then evaluated to obtain the updated mean component and marginal covariance matrix.

In addition, the GBMixed framework provides a choice of base learners for each model component. Learners may range from simple intercept-only models, which yield constant (homogeneous) updates, to more flexible techniques. Linear models such as ordinary least squares are appropriate when a parametric structure is assumed or desired for interpretability. More flexible alternatives, including multivariate adaptive regression splines (MARS; Friedman 1991), allow for smooth, nonlinear effects and low-order interactions through piecewise linear splines with automatic knot selection. Decision trees or classification

and regression trees (CART; Breiman et al. 1984) offer a nonparametric and highly adaptable option, capable of capturing complex interaction structures, handling mixed-type inputs (including missing values for covariates), and exhibiting robustness to outliers. The same design flexibility applies to variance components as with the mean, although these are typically modeled using simpler learners such as linear regression or low-complexity trees to enable interpretation and maintain stability in high-dimensional variance estimation, while avoiding overfitting the variance structure. This modularity allows the algorithm to span a range of model classes, from parametric formulations to fully nonparametric clustered data models.

4.5 Variants: GBMixed-Base, GBoost, RBoost and GRBoost

The overarching GBMixed framework provides a modular structure for building a wide range of mixed models. By specifying a base learner for each of the three core components, the mean function $f(\cdot)$, the random effects variance \mathbf{G}_i , and the residual variance \mathbf{R}_i , users can recover traditional models as special cases or define new classes of nonparametric, heteroscedastic, or clustered data models with covariate-dependent variance.

Table 1: Model configurations under the GBMixed framework based on learner choices for mean, residual variance, and random effects variance.

Mean $h_\mu^{(m)}$	Residual Variance $h_R^{(m)}$	Random Variance $h_G^{(m)}$	Model Class
OLS	Constant	Constant	Linear Mixed Model (LMM)
Nonparametric	None	None	Gradient Boosting Machine (GBM)
Nonparametric	Constant	Constant	GBMixed-Base baseline (nonparametric mean)
Nonparametric	Nonparametric	Constant	RBoost : heteroscedastic residual variance
Nonparametric	Constant	Nonparametric	GBoost : heterogeneous random effects variance
Nonparametric	Nonparametric	Nonparametric	GRBoost : joint heterogeneous variance

Each row in the table represents a model variant within the framework, defined by the functional form of its components. The simplest case, where the mean is boosted linearly via ordinary least squares and the residual variance and random variance via a constant update (gradient ascent) we recover standard linear mixed models. Using nonparametric base learners for the mean (e.g., trees or splines) and no updates for the variance components yields a gradient boosting machine. Incorporating a homogeneous variance structure for residual and random effects components (via constant mean updates) delivers the GBMixed-Base variant. Introducing nonparametric learners for the variance components leads to richer model classes that adapt the covariance structure to covariates. In fact, parametric learners can also be used for the variance components to deliver heterogeneous variance models, if interpretability is preferred.

We define three variants beyond the baseline GBMixed model. The *RBoost* variant permits the

residual variance to vary across observations. Here, the diagonal residual covariance matrix $\log \mathbf{R}_i$ is modeled via gradient boosting using observation-level features. This formulation captures heteroscedastic noise patterns, common in applications where measurement error depends on subject characteristics or context. It also allows for classical heteroscedastic fanning of residuals vs predictions, commonly observed when an alternative error distribution might be required for the response.

In contrast, the *GBoost* variant models group-specific random effects variances as functions of group-level covariates. This structure enables stable and interpretable random effects variance modeling across heterogeneous groups, such as hospitals, regions, or institutions. As outlined earlier, for each group i , the random effects covariance matrix \mathbf{G}_i can be parameterized via a Cholesky decomposition, $\mathbf{G}_i = \mathbf{L}_i \mathbf{L}_i^\top$ and in that case boosting updates are applied to the lower triangle entries of \mathbf{L}_i instead of \mathbf{G}_i directly.

The most general variant, *GRBoost*, combines both of these extensions. It simultaneously models covariate-dependent residual variances and random effects variances, producing a covariance structure for each group i , of the form $\Sigma_i = \mathbf{Z}_i \mathbf{G}_i \mathbf{Z}_i^\top + \mathbf{R}_i$, where \mathbf{R}_i is assumed to be diagonal. Boosting is applied to both \mathbf{L}_i and $\log R_{ij}$, ensuring strictly positive variance predictions via unconstrained optimization. While the current implementation assumes uncorrelated residual variances, the GBMixed framework could be extended to a structured or full \mathbf{R}_i matrix in future work.

All variants operate within the same algorithmic infrastructure. The base learners for each component are fit to the likelihood-based gradients and updated via gradient boosting using separate learning rates. Crucially, the updating of all components occurs in parallel, ensuring that no component dominates or biases convergence. This structure permits different base learner choices depending on desired model complexity or computational constraints. For instance, trees may be used to capture nonlinear treatment interactions in the mean, while linear models or shallow trees (e.g., trees with depth one or two) may be preferred for stable variance estimation. These simpler base learners reduce the risk of overfitting to noisy gradient signals, which is particularly important when modeling variance components.

In summary, the overarching GBMixed framework incorporates a number of existing models as reference points (linear mixed models and gradient boosting machines), as well as a number of extensions for incorporating variance decomposition (potentially heterogeneous) with gradient boosting.

4.6 Regularization and Convergence

Regularization mechanisms are applied to ensure stable convergence and prevent overfitting. Each component update is scaled by a learning rate (ν_μ for the mean function, ν_G for the random effects covariance, and ν_R for the residual variance) controlling the size of each boosting step. At every iteration, a random subset of groups (proportion π) and covariates (proportion ξ) are selected, introducing stochastic elements that act as an implicit form of bagging, improving generalization and reducing modeling variance.

To determine convergence, the algorithm monitors the held-out log-likelihood across iterations, ℓ .

Iteration stops when the improvement over a look-back window k falls below a fixed threshold δ , that is, when $|\ell^{(m)} - \ell^{(m-k)}| < \delta$. This early stopping criterion prevents unnecessary computation once the model is saturated and balances fit against complexity.

When boosting is applied with squared error loss, the procedure corresponds to functional gradient descent and convergence is guaranteed under certain conditions (see Bühlmann and Yu, 2003 and Zhang and Yu, 2005). In the likelihood-based formulation used here, the updates are equivalently viewed as functional gradient ascent on the log-likelihood, as in NGBoost (Duan et al., 2019).

In summary, shrinkage, subsampling, and convergence control stabilize estimation and limit overfitting for more consistent convergence.

4.7 Prediction, Uncertainty and Inference

4.7.1 Response Prediction and Uncertainty Estimation

Once the model training has converged, predictions and associated uncertainty can be derived using the estimated mean and variance components. This section describes how the GBMixed algorithm outputs are used to produce predictions with random effects and quantify prediction uncertainty.

Predictions for new data are made by combining the estimated mean function $\hat{f}^{(M)}$ with subject-specific random effect adjustments. These adjustments can be computed using the Best Linear Unbiased Prediction (BLUP) formula, which leverages the estimated variance components $\hat{\mathbf{G}}_i$ and $\hat{\mathbf{R}}_i$ to optimally recover latent group-level signals from the data. The resulting predictions incorporate both the global structure learned by $\hat{f}^{(M)}$ and local deviations at the group level captured by the BLUPs, with the influence of each group-level adjustment scaled according to the fitted \mathbf{G}_i . In models such as *GBoost* and *GRBoost*, where \mathbf{G}_i varies with covariates, this allows the degree of group-level shrinkage to adapt to the characteristics of each group, enabling stronger or weaker local adjustment depending on the evidence in the training data and generally driving better test data prediction accuracy.

For a group i with design matrix \mathbf{Z}_i and residual vector $\hat{\mathbf{e}}_i = \mathbf{y}_i - \hat{f}^{(M)}(\mathbf{X}_i)$, the random effects are estimated as:

$$\hat{\mathbf{u}}_i = \hat{\mathbf{G}}_i \mathbf{Z}_i^\top \hat{\Sigma}_i^{-1} \hat{\mathbf{e}}_i,$$

where $\hat{\Sigma}_i = \mathbf{Z}_i \hat{\mathbf{G}}_i \mathbf{Z}_i^\top + \hat{\mathbf{R}}_i$ is the group-specific covariance matrix. When heterogeneous variance models are used, the variance components $\hat{\mathbf{G}}_i$ and $\hat{\mathbf{R}}_i$ are obtained by evaluating the learned functions $\hat{H}_{\mathbf{G}}^{(M)}$ and $\hat{H}_{\mathbf{R}}^{(M)}$.

To estimate predictions of the mean response for a new observation j from group i , incorporating these random effects, we compute:

$$\hat{\mu}_{ij|\mathbf{u}_i} = \hat{f}^{(M)}(\mathbf{x}_{ij}) + \mathbf{z}_{ij}^\top \hat{\mathbf{u}}_i = \mathbb{E}[Y_{ij} \mid \mathbf{x}_{ij}, \mathbf{u}_i]. \quad (4.1)$$

The mean estimate $\hat{\mu}_{ij}$ represents the population-average response for a given covariate profile, while $\hat{\mu}_{ij|\mathbf{u}_i}$ incorporates group-specific deviations through the random effects \mathbf{u}_i .

For new or unobserved groups, random effects cannot be estimated directly and hence predictions default to the fixed effect component by setting $\hat{\mathbf{u}}_i = \mathbf{0}$.

Having defined the point-prediction approach, the total variance of Y_{ij} is given by

$$\text{Var}(Y_{ij}) = \mathbf{z}_{ij}^\top \mathbf{G}(\tilde{\mathbf{x}}_i) \mathbf{z}_{ij} + R(\mathbf{x}_{ij})$$

as in Equation (3.6). This decomposition accounts for conditional predictive variance under the fitted mixed model due to both random effects and residual error. The term $\mathbf{z}_{ij}^\top \mathbf{G}(\tilde{\mathbf{x}}_i) \mathbf{z}_{ij}$ captures within-group correlation (random effects), while $R(\mathbf{x}_{ij})$ represents individual-level variation (residual error).

Using this variance expression, prediction intervals can be constructed to quantify uncertainty in new outcomes. For an observation j from group i , the approximate $(1 - \alpha)$ prediction interval is

$$Y_{ij} \in \left[\hat{\mu}_{ij} \pm z_{1-\alpha/2} \sqrt{\text{Var}(Y_{ij})} \right]$$

When modeling new groups with no random effect adjustments, the variance reduces to $\text{Var}(Y_{ij}) = \hat{R}(\mathbf{x}_{ij})$, the standard form of an individual prediction interval.

4.7.2 Conditional Average Treatment Effect (CATE)

Treatment effects can be incorporated by including a binary (or multi-level) treatment indicator T_{ij} alongside the covariates of \mathbf{x}_{ij} as a fixed effect. This allows the model to recover heterogeneous treatment effects across subgroups rather than imposing a constant effect. Formally, for a binary treatment, let $Y_{ij}(t) \in \mathbb{R}$ denote the potential outcome for observation (i, j) under the treatment level t . The Conditional Average Treatment Effect (CATE) for the observation covariates \mathbf{x}_{ij} is defined as

$$\text{CATE} = \tau(\mathbf{x}_{ij}) = \mathbb{E}[Y_{ij}(1) - Y_{ij}(0) \mid \mathbf{x}_{ij}],$$

and is estimated by

$$\hat{\tau}(\mathbf{x}_{ij}) = \hat{f}^{(M)}(\mathbf{x}_{ij}, t = 1) - \hat{f}^{(M)}(\mathbf{x}_{ij}, t = 0),$$

where $\hat{f}^{(M)}(\mathbf{x}_{ij}, t = 1)$ and $\hat{f}^{(M)}(\mathbf{x}_{ij}, t = 0)$ denote the fitted mean components under treatment and control, respectively. This approach naturally includes the special case of a constant treatment effect, while also enabling flexible estimation of heterogeneous effects through interactions between treatment and other covariates. See, for example, (Wager and Athey, 2017).

More generally, when T_{ij} is continuous (e.g., dosage or intensity), the model captures a response

function for the treatment

$$\tau(t \mid \mathbf{x}_{ij}) = \frac{\partial}{\partial t} \mathbb{E}[Y_{ij}(t) \mid \mathbf{x}_{ij}] = \frac{\partial}{\partial t} f(\mathbf{x}_{ij}, t),$$

which represents the incremental change in the fitted mean component with respect to the continuous treatment variable t . These CATEs provide a view of how treatment effects vary across the covariate space. In the GBMixed framework, $f(\mathbf{x}_{ij}, t)$ is learned via gradient boosting and can capture nonlinear and interaction effects between treatment and covariates, therefore providing heterogeneous treatment effects.

While the CATE quantifies the expected treatment effect at given covariates, it represents only the mean of the underlying distribution of individual treatment responses. To understand the variability of treatment responses around this mean, it is useful to consider the individual treatment effects (ITEs) and their variance.

$$\text{ITE} = \Delta_{ij} = Y_{ij}(1) - Y_{ij}(0),$$

represents the realized difference between the potential outcomes under treatment and control, although both potential outcomes are generally not jointly observable. The expected values of CATE and ITE are the same however they differ in how uncertainty is interpreted. The variance of CATEs reflects the uncertainty in the expected treatment effect for an individual, whilst the variance of the ITEs reflects the variance in the full realized outcome, including any residual error. In other words, the CATE variance describes the treatment effect uncertainty alone, while the ITE variance quantifies the total uncertainty in realized outcomes under treatment versus control.

The variance of the ITE can be expressed as

$$\text{Var}[\Delta_{ij} \mid \mathbf{x}_{ij}] = \text{Var}[Y_{ij}(1) \mid \mathbf{x}_{ij}] + \text{Var}[Y_{ij}(0) \mid \mathbf{x}_{ij}] - 2 \text{Cov}[Y_{ij}(1), Y_{ij}(0) \mid \mathbf{x}_{ij}],$$

where $\text{Var}[Y_{ij}(t) \mid \mathbf{x}_{ij}]$ is given by Equation (3.6). When a random-slope for treatment is included in the model, the variance under treatment includes both the random intercept and random slope components, while the variance under control includes only the random intercept. The covariance term arises from the covariance between the random intercept and slope and can be written as

$$\text{Cov}[Y_{ij}(1), Y_{ij}(0) \mid \mathbf{x}_{ij}] = \mathbf{z}_{ij}^\top \hat{\mathbf{G}}_{10}(\tilde{\mathbf{x}}_i) \mathbf{z}_{ij},$$

where $\hat{\mathbf{G}}_{10}$ denotes the estimated cross-covariance between the random effects for treatment and control. If the model includes no random slope for the treatment effect, this covariance term is assumed to be zero.

In addition, this decomposition extends naturally to multi-level or continuous treatments. For discrete

treatments $t \in \{0, 1, \dots, K\}$, the variance of the individual effect comparing levels t_a and t_b is

$$\text{Var}[\Delta_{ij}(t_a, t_b) \mid \mathbf{x}_{ij}] = \text{Var}[Y_{ij}(t_a) \mid \mathbf{x}_{ij}] + \text{Var}[Y_{ij}(t_b) \mid \mathbf{x}_{ij}] - 2 \text{Cov}[Y_{ij}(t_a), Y_{ij}(t_b) \mid \mathbf{x}_{ij}].$$

For continuous treatments, an equivalent measure is the variance of the marginal treatment effect $\Delta'(t) = \partial Y(t) / \partial t$, which can be approximated by incremental differences of the same form as above.

Using the point prediction and variance estimates for the treatment effects, we can construct approximate prediction intervals describing the expected variation in individual treatment effects:

$$\Delta_{ij} \in \left[\tau(\mathbf{x}_{ij}) \pm z_{1-\alpha/2} \sqrt{\text{Var}(\Delta_{ij} \mid \mathbf{x}_{ij})} \right].$$

This interval represents the dispersion of potential outcomes around the mean, providing an approximate coverage range for realized treatment effects.

4.7.3 Average Treatment Effect (ATE)

The Average Treatment Effect (ATE) quantifies the expected difference between potential outcomes across the entire population. It is defined as

$$\text{ATE} = \mathbb{E}[\Delta] = \mathbb{E}[Y(1)] - \mathbb{E}[Y(0)] = \mathbb{E}_{\mathbf{X}}[\tau(\mathbf{X})],$$

where $\tau(\mathbf{X}) = \mathbb{E}[Y(1) - Y(0) \mid \mathbf{X}]$ denotes the conditional average treatment effect.

In practice, the ATE can be estimated by averaging the predicted treatment and control differences across the sample:

$$\widehat{\text{ATE}} = \frac{1}{N} \sum_{i=1}^C \sum_{j=1}^{n_i} [\hat{f}^{(M)}(\mathbf{x}_{ij}, 1) - \hat{f}^{(M)}(\mathbf{x}_{ij}, 0)],$$

which provides a population-level summary of the overall treatment impact, analogous to the treatment coefficient in a linear mixed model.

Estimating the sampling variance of the ATE depends critically on the study design, model structure, and assumptions about independence. In simple randomized experiments with independent units, constant treatment effects and unadjusted difference estimator, the variance can be computed directly using classical formulas. However, in more complex studies, estimation becomes substantially more difficult without heavily simplifying assumptions. We are interested in cases where there are complex covariance structures requiring calculation of joint covariances across predictions, which would be computationally intensive and generally intractable. In addition, we are also most interested in heterogeneous treatment effects rather than population averaged effects and as such, the ATE is less informative.

4.7.4 Implications for Inference and Causal Estimation

Inference from GBMixed arises from several model components. The estimated random effects and residual error estimates, even under homogeneous variance models, provide meaningful insights for understanding the data-generating process. The individual response predictions with and without random effect adjustments provide greater accuracy in point estimation and also when combined with the associated variance estimates, they provide the full probabilistic outcomes. These are useful in many applications requiring prediction intervals, quantile estimation, or risk aware decision making under uncertainty.

The CATE estimates further support individualized inference by characterizing how treatment effects vary across covariates, while also providing a full probabilistic outcome of the expected response. It therefore allows practitioners to assess not only where and for whom treatment is likely to be effective, but also uncertainty quantification around that estimate. These quantities are important for applications requiring personalized decisions, such as targeted interventions, precision medicine, or policy prioritization based on heterogeneous effects.

Under the potential outcomes framework (Rubin, 1974; Holland, 1986), each observational unit is assumed to have two potential outcomes: treatment, $Y_{ij}(1)$, and control, $Y_{ij}(0)$, though only one of these is observed. The causal effect for an individual is defined as the difference between these potential outcomes, and the Conditional Average Treatment Effect (CATE) is the expected value of this difference given covariates.

In this framework, the estimated CATEs from GBMixed can be interpreted as causal treatment effects, provided standard assumptions hold. Specifically, $\tau(\mathbf{x}_{ij})$ corresponds to the conditional average treatment effect if (i) treatment assignment is unconfounded given covariates; and (ii) there is sufficient overlap in treatment assignment, meaning individuals with similar covariate profiles appear in both treatment and control groups.

4.8 Model Diagnostics: Variable Importance and Partial Dependence Plots

To interpret the fitted GBMixed models, we use two standard diagnostics from the gradient boosting literature: variable importance and partial dependence plots (Friedman, 2001; Chen and Guestrin, 2016). We also extend these tools to the variance components, providing novel insights into heteroscedasticity and group-level heterogeneity.

4.8.1 Variable Importance

Variable importance quantifies the contribution of each covariate to model predictions. Two common measures exist: (i) the total reduction in loss function attributable to each variable across all splits, and (ii) the frequency with which each variable is selected across boosting iterations. We adopt the frequency

measure for computational simplicity and interpretability across diverse base learner types. Specifically, we compute:

$$\text{Importance}(x_j) = \frac{1}{M} \sum_{m=1}^M \text{Count}(x_j, m),$$

where M is the total number of boosting iterations and $\text{Count}(x_j, m)$ is the number of splits (trees) or basis functions (MARS) using variable x_j in iteration m . This importance is normalized by dividing each frequency by the sum of importance across all covariates.

4.8.2 Partial Dependence Plots

Partial dependence plots visualize the marginal effect of a covariate on model predictions by averaging over the distribution of other covariates. For covariate x_s , the partial dependence function is:

$$\hat{f}_s(x_s) = \frac{1}{n} \sum_{i=1}^n \hat{f}(x_s, \mathbf{x}_{i,\setminus s}),$$

where $\mathbf{x}_{i,\setminus s}$ denotes all covariates except x_s . When x_s interacts with other variables, the plot reflects the average effect across those interaction patterns. For models with strong interactions, joint partial dependence plots for pairs of variables provide richer diagnostics.

4.8.3 Extension to Variance Components

A novel contribution of GBMixed is the application of these diagnostics to variance components $\hat{H}_G^{(M)}$ and $\hat{H}_R^{(M)}$. Variable importance for \hat{H}_R identifies which covariates drive residual heteroscedasticity, while importance for \hat{H}_G reveals which group-level covariates affect random effects variance. Partial dependence plots for variance components show how variability changes across the covariate space, which represent patterns invisible in models with constant variance assumptions. These diagnostics provide interpretable summaries of potentially complex covariance structures and assist in understanding the drivers of heterogeneity in hierarchical data.

5 Experiments

5.1 Objectives and Setup

We evaluate three controlled simulation scenarios that progressively introduce challenges common in statistical inference: (i) accuracy in recovering conditional average treatment effects (CATEs), (ii) uncertainty quantification, and (iii) recovery of variance components under covariate dependence, with interpretability assessed via variable importance and partial dependence diagnostics.

The experiment designs build on the heterogeneous treatment effect framework of (Wager and Athey, 2017), extended to clustered data with nonlinear outcomes and covariate-dependent variance components.

In each scenario, data are generated from a fixed data-generating process with known CATE, clusters are randomly split 60/40 into training and test sets, and performance is evaluated on the held-out test data. We compare GBMixed against ordinary least squares (OLS; `stats::lm`), linear mixed-effects regression (LMER; `lme4::lmer`), random forest (RF; `ranger::ranger`), gradient boosting with XGBoost (XGB; `xgboost::xgboost`; Chen and Guestrin 2016), and causal forest (CF; `grf::causal_forest`). Each scenario is replicated 100 times. Full data-generating processes, hyperparameters, and additional diagnostics are provided in Appendix B.

We assess accuracy of the CATEs using mean squared error (MSE). For uncertainty quantification, OLS, LME, and CF report empirical coverage of 90% confidence intervals for the CATE. In comparison, GBMixed reports empirical coverage of 90% prediction intervals for the realized treatment contrast ($Y_1 - Y_0$), which incorporates both residual and random-effect variability. This ensures that interval coverage is evaluated on comparable like-for-like targets for each approach, using the uncertainty estimation that they are each designed for. RF and XGB do not provide any uncertainty estimates and as such have no coverages calculated.

5.2 Experiment A: Nonlinear matched pairs with heterogeneous treatment effects and random Intercepts

This scenario builds a complex modeling problem with 300 predictors that mix Gaussian and non-Gaussian types (uniform, Bernoulli, Poisson), across $n = 10,000$ observations split 60 / 40 for training and testing. The hierarchical response model is given by

$$y_{ij} = \alpha_i + m(x_{ij}) + \tau(x_{ij}) w_{ij} + \epsilon_{ij}, \quad \alpha_i \sim \mathcal{N}(0, \sigma_\alpha^2), \quad \epsilon_{ij} \sim \mathcal{N}(0, \sigma_\epsilon^2),$$

where $m(\cdot)$ defines the nonlinear baseline function and $\tau(\cdot)$ the treatment effect function. Specifically,

$$m(x_{ij}) = 0.5 \sin(x_{ij,1}) + 0.1 x_{ij,2}^2 + 0.1 x_{ij,3} x_{ij,4} + 0.3 \log(x_{ij,4} + 1) x_{ij,5} + x_{ij,1} x_{ij,5},$$

and

$$\tau(x_{ij}) = \varsigma(x_{ij,6}) \varsigma(x_{ij,7}), \quad \varsigma(x) = \frac{1}{1 + e^{-20(x-1/3)}}.$$

Observations are organized as matched pairs with a single group-level random intercept to induce within-cluster dependence, and both the random intercept and the residual error are homoscedastic.

This design isolates treatment-effect heterogeneity (not variance heterogeneity) and tests whether methods recover accurate CATEs and still estimate well-calibrated uncertainty intervals. Table 2 reports the headline metrics. GBMixed attains the best CATE MSE (0.0605) with coverage close to 90% (87.3%), while methods that ignore heterogeneous treatment effects (OLS/LMER) perform poorly

Table 2: Experiment A CATE mean squared error (MSE) and coverage (%).

Method	CATE MSE (\pm SD)	Coverage (%) (\pm SD)
OLS	0.9914 (0.0208)	2.8 (0.5)
LMER	0.9914 (0.0208)	1.4 (0.4)
RF	0.0948 (0.0230)	—
XGB	0.4496 (0.0625)	—
CF	0.7182 (0.0298)	8.8 (0.9)
GBMixed	0.0605 (0.0122)	87.3 (1.7)

Note: Coverage for GBMixed refers to 90% prediction intervals. Others are 90% confidence intervals.

and nonparametric baselines (RF/XGB) improve prediction somewhat but do not provide calibrated intervals. CF delivers poor CATE accuracy and substantially underestimates uncertainty in this setting.

Figure 2 shows test-set CATE predictions versus ground truth for a representative replication, across models. Once again, it is clear that GBMixed delivers the closest match to the ground truth, also providing a reasonably consistent range of residual errors across the predictions.

Full details of the experiment are in Appendix B.1.

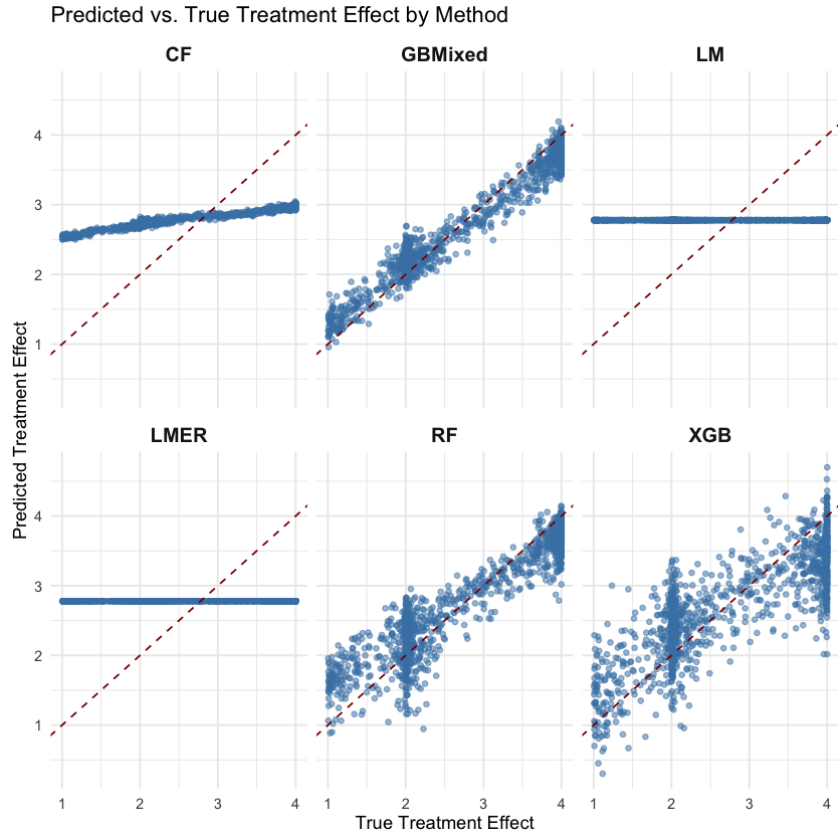


Figure 2: Experiment A Test-set CATE predictions vs ground truth for a representative replication.

5.3 Experiment B: Covariate-dependent residual variance

This scenario builds on Experiment A but replaces constant residual noise with a covariate-dependent error structure. We generate 30 predictors (all uniform on $[0, 1]$) and $n = 10,000$ observations split 60 / 40, retain matched pairs with a homoscedastic random intercept to induce within-cluster dependence, and set a simple mean function. Residual variance increases away from the midpoint of x_2 (a V-shape) and exhibits a step change at $x_5 \geq 0.5$. The treatment effect remains heterogeneous and interaction-driven (via sigmoids of x_1 and x_2).

The hierarchical response model is

$$y_{ij} = \alpha_i + m(x_{ij}) + \tau(x_{ij}) w_{ij} + \epsilon_{ij}, \quad \alpha_i \sim \mathcal{N}(0, \sigma_\alpha^2), \quad \epsilon_{ij} \sim \mathcal{N}(0, R(\mathbf{x}_{ij})),$$

where $w_{ij} \in \{0, 1\}$ denotes treatment assignment within matched pairs. The baseline and treatment functions are defined as

$$m(x_{ij}) = 2x_{ij,1} + 1, \quad \tau(x_{ij}) = \varsigma(x_{ij,1}) \varsigma(x_{ij,2}), \quad \varsigma(x) = \frac{1}{1 + e^{-20(x-1/3)}}.$$

Residual variance varies systematically with covariates,

$$R(x_{ij}) = 0.3 + 0.4 |x_{ij,2} - 0.5| + 0.4 \mathbf{1}(x_{ij,5} \geq 0.5),$$

creating both continuous and discrete heteroscedasticity patterns that challenge models assuming constant variance. The random intercept variance is set to $\sigma_\alpha^2 = 0.25$.

This design tests whether methods can recover $R(\cdot)$ while maintaining CATE accuracy and coverage. Table 3 reports CATE MSE, coverage, and R -MSE. GBMixed (RBoost) continues to excel at CATE accuracy (0.0047) and maintains coverage near the 90% target (88.3%). Crucially, it also recovers the residual variance surface with the lowest R -MSE (0.0163 vs 0.0633 for LMER), confirming that the learner algorithms can be applied to variance components to uncover structure. CF delivers the second best CATE error but its confidence-interval coverage remains below the nominal 90%.

Table 3: Experiment B: CATE mean squared error (MSE), coverage (%), and residual-variance R MSE.

Method	CATE MSE (\pm SD)	Coverage (%) (\pm SD)	R_{ij} MSE
OLS	0.0101 (0.0004)	10.3 (2.8)	—
LMER	0.0101 (0.0004)	7.8 (1.4)	0.0633
RF	0.0128 (0.0027)	—	—
XGB	0.0213 (0.0049)	—	—
CF	0.0078 (0.0009)	67.5 (4.8)	—
RBoost	0.0047 (0.0011)	88.3 (1.0)	0.0163

Note: Coverage for GBMixed refers to 90% prediction intervals. Others are 90% confidence intervals.

Figure 3 shows partial-dependence diagnostics that mirror the data-generating variance pattern. Full details appear in Appendix B.2.

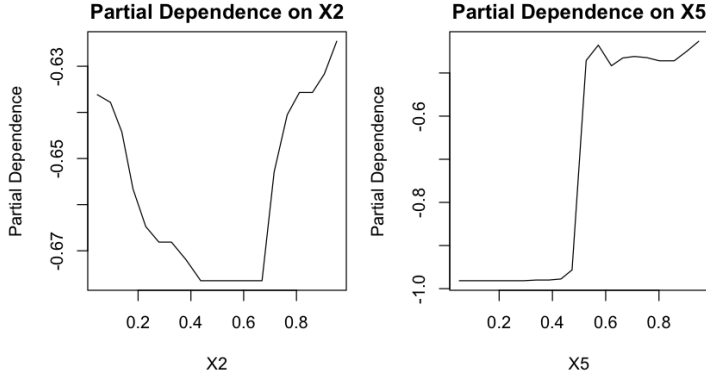


Figure 3: Partial dependence of residual variance on x_2 (left: V-shape) and x_5 (right: step) for a representative replication.

5.4 Experiment C: Joint covariate heterogeneity in residual and random effects variance

This scenario extends Experiment B by allowing both variance components to vary with covariates. We retain matched pairs and a simple mean function, keep the random intercept, and introduce covariate-dependent heterogeneity at both levels: residual variance varies with x_5 and the random–effect variance varies with a group-level covariate (e.g., \tilde{x}_3). The treatment effect remains nonlinear and interaction-driven.

Covariates are simulated as $x_{1:30} \sim U(0, 1)$, with $n = 10,000$ total observations and $p = 30$ predictors. Sixty percent of observations are used for training and forty percent for held-out testing. The hierarchical response model is

$$y_{ij} = \alpha_i + m(x_{ij}) + \tau(x_{ij}) w_{ij} + \epsilon_{ij}, \quad \alpha_i \sim \mathcal{N}(0, G(\tilde{\mathbf{x}}_i)), \quad \epsilon_{ij} \sim \mathcal{N}(0, R(\mathbf{x}_{ij})),$$

where $w_{ij} \in \{0, 1\}$ denotes treatment assignment within matched pairs. The baseline and treatment functions are defined as

$$m(x_{ij}) = 2x_{ij,1} + 1, \quad \tau(x_{ij}) = \varsigma(x_{ij,1}) \varsigma(x_{ij,2}), \quad \varsigma(x) = \frac{1}{1 + e^{-20(x-1/3)}}.$$

The variance components vary systematically with covariates,

$$R(\mathbf{x}_{ij}) = 0.4 + 0.4 |x_{ij,5} - 0.5|, \quad G(\tilde{\mathbf{x}}_i) = 0.5 + 1.5 |\tilde{x}_{i,3} - 0.5|,$$

creating covariate-dependent structures for both within-group and between-group variability.

Table 4 reports CATE MSE, coverage, and variance-recovery metrics. GBMixed (GRBoost) again achieves the best CATE MSE (0.0057) with near-nominal prediction-interval coverage (89.3%). It recovers both variance components accurately, with the lowest R -MSE (0.0148) and G -MSE (1.9888) compared to LMER (restricted to homogeneous variance). CF shows again the second strongest CATE accuracy and higher confidence-interval coverage.

Table 4: Experiment C: CATE mean squared error (MSE), coverage (%), residual-variance R MSE, and random-effect variance G MSE.

Method	CATE MSE (\pm SD)	Coverage (%) (\pm SD)	R_{ij} MSE	G_i MSE
OLS	0.0101 (0.0003)	30.9 (10.3)	—	—
LMER	0.0101 (0.0003)	7.8 (1.2)	0.0578	3.5223
RF	0.0383 (0.0052)	—	—	—
XGB	0.0332 (0.0065)	—	—	—
CF	0.0092 (0.0005)	93.8 (1.3)	—	—
GRBoost	0.0057 (0.0012)	89.3 (1.1)	0.0148	1.9888

Note: Coverage for GBMixed refers to 90% prediction intervals. Others are 90% confidence intervals.

Figure 4 shows variable-importance diagnostics for the residual and random-effect variance learners demonstrating that these model diagnostics correctly identify the covariates driving each variance component. Full details appear in Appendix B.3.

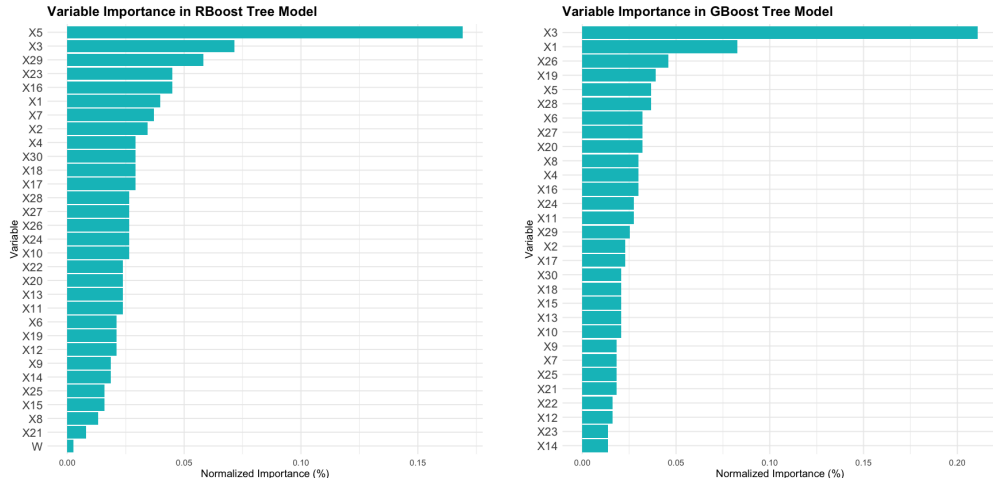


Figure 4: Variable importance for residual variance (left, RBoost) and random-effect variance (right, GBoost) for a representative replication. The dominant drivers align with the data-generating variance patterns.

5.5 Cross-experiment summary

Across these experiments, GBMixed delivers the lowest CATE error and stable, near-nominal 90% coverage. Overall, the experiments show that GBMixed consistently outperforms alternative methods in

CATE estimation, particularly in complex nonlinear and clustered data settings. In addition, it achieves reliable coverage across all designs, demonstrating its ability to accurately estimate variance components and provide well-calibrated uncertainty quantification. Finally, GBMixed uniquely recovers heterogeneous variance structures, yielding accurate estimates of both group-level covariate-dependent random effects variances (\mathbf{G}) and observation level covariate-dependent residual variances (R).

6 Applications

6.1 Predicting Longitudinal Liver Biomarkers in Primary Biliary Cirrhosis (PBC)

The primary biliary cirrhosis (PBC) dataset from the Mayo Clinic trial is a benchmark in the survival and clinical modeling literature (Fleming and Harrington, 1991). It contains longitudinal measurements on 312 patients with advanced liver disease, resulting in 1,945 observations in total. The clustered structure arises from repeated visits per patient, with measurements on treatment assignment (D-penicillamine vs placebo), demographics, and biochemical markers. This dataset provides a challenging test case with clustered structure (visits nested within patients), heterogeneous disease trajectories, and nonlinear relationships among biochemical covariates. A detailed description of preprocessing, missing-data handling, and baseline model specification is provided in Appendix C.

Table 5: Comparison of model performance (train and test mean squared error, MSE) across all methods and treatment groups for the PBC dataset. Treatment: N = placebo, Y = D-penicillamine.

Dataset	Treatment	OLS	LMER	GBMixed (OLS)	GBMixed (MARS)	Random Forest	XGBoost
Train	All	0.1728	0.0698	0.0688	0.0499	0.0234	0.0662
Train	N	0.1705	0.0608	0.0598	0.0425	0.0227	0.0699
Train	Y	0.1751	0.0787	0.0777	0.0572	0.0241	0.0625
Test	All	0.2536	0.1631	0.1632	0.1390	0.1568	0.1643
Test	N	0.2350	0.1289	0.1291	0.0979	0.1003	0.1147
Test	Y	0.2725	0.1980	0.1981	0.1810	0.2145	0.2150

We model the log-transformed serum glutamic oxaloacetic transaminase (SGOT or AST) biomarker as the response, using key clinical covariates as predictors and including treatment assignment as a covariate. For each patient with multiple visits, we include all but their last observation in the training set, while reserving their final observation for the test set resulting in 1660 training observations and 285 test observations. Single observation patients are included in the training set only. As a baseline, we fit a linear mixed-effects model with random intercepts (after testing and finding minimal slope variation) to account for within-patient correlation. This model achieves strong predictive accuracy on held-out records (Table 5, test MSE = 0.163). We then apply GBMixed (with homogeneous variance) in two configurations: first with OLS base learners (for the mean component) to confirm equivalence with the

mixed-effects model, and second with multivariate adaptive regression splines (MARS) base learners to capture potential nonlinear effects and interactions. The MARS version of GBMixed reduces test error to 0.139, outperforming both the LMER baseline and nonparametric machine learning comparators (random forest and XGBoost), which do not account for clustered structure.

When using GBMixed, the treatment indicator does not enter as a predictor (has zero variable importance), and the model attains higher predictive accuracy for both treated and control patients. This suggests that once nonlinear and interaction effects are captured for other covariates, treatment assignment contributes little additional explanatory power.

Among the biochemical markers, alkaline phosphatase (`alk.phos`) and bilirubin (`bili`) emerge as dominant predictors, shown in Figure 5.

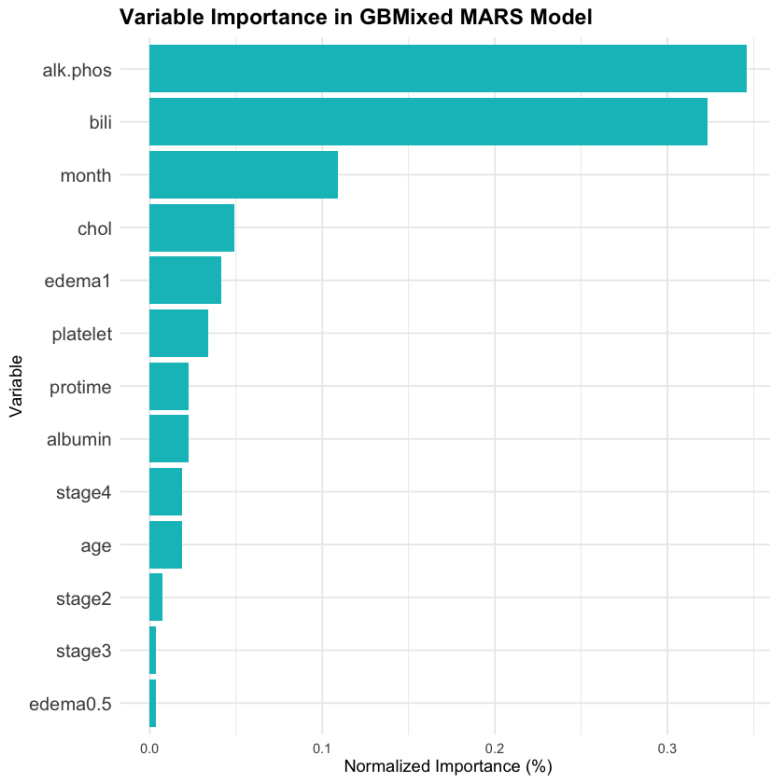


Figure 5: Variable importance from GBMixed with MARS base learners. Alkaline phosphatase, bilirubin, prothrombin time, cholesterol, and albumin rank as the top predictors, motivating closer inspection through partial dependence plots.

Building on these results, we examine partial dependence plots to visualize nonlinear effects. From a clinical perspective, the nonlinear effects of alkaline phosphatase and bilirubin (Figure 6) highlight their role as biomarkers of disease severity demonstrating decreasing effects for higher levels.

Figure 7 shows clear curvature for platelet count (`platelet`) and cholesterol (`chol`), both of which exhibit nonlinear risk trajectories. Platelet count displays a distinct “V”-shaped relationship, indicating elevated SGOT levels for both abnormally low and high values. In contrast, cholesterol increased linearly till about halfway and then reverses. The ability of GBMixed to uncover these patterns provides evidence

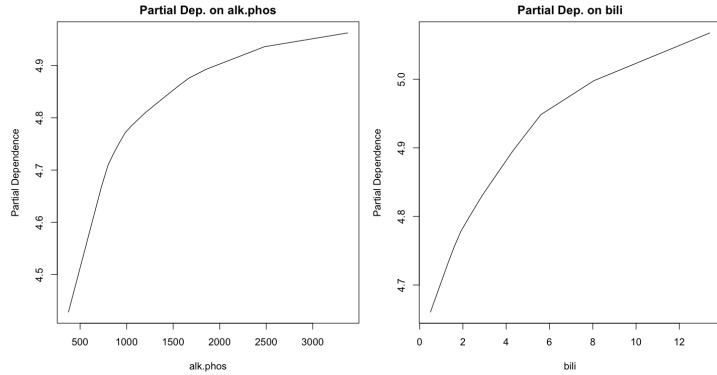


Figure 6: Partial dependence plot from GBMixed (MARS base learners) showing the nonlinear effect of alkaline phosphatase on log(SGOT).

that flexible modeling of biomarker trajectories may improve monitoring and treatment evaluation in chronic liver disease.

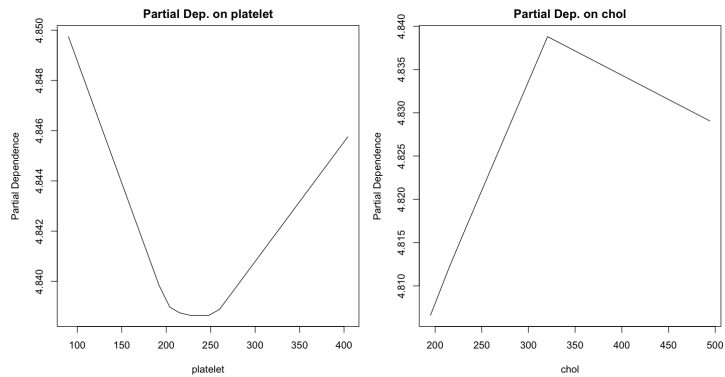


Figure 7: Partial dependence plots for GBMixed with MARS base learners. Left: nonlinear effect for platelet count; Right: nonlinear effect for patient age.

We can also use the GBMixed models to identify interaction effects by examining the individual base learner models. A strong interaction is observed between alkaline phosphatase and prothrombin time (Figure 8), where the prothrombin effect is steeper at lower levels of alkaline phosphatase. This suggests that combinations of markers contribute jointly to disease severity.

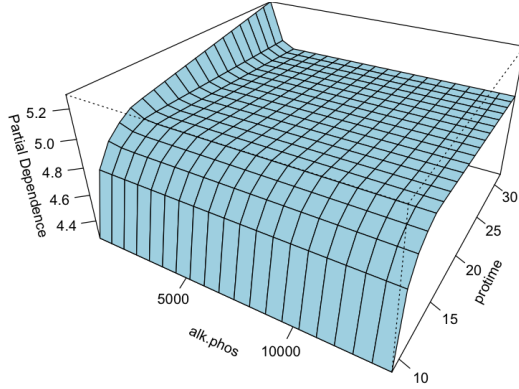


Figure 8: Three-dimensional partial dependence plot from GBMixed with MARS base learners. Interaction between alkaline phosphatase and prothrombin time

In summary, the PBC application illustrates that GBMixed reconciles with linear mixed-effects models under parametric specifications, while delivering superior predictive accuracy and richer insights when flexible base learners are employed. Additional diagnostic results, including fixed-effect estimates, random effects variances, variable importance measures, and partial dependence plots, are reported in Appendix C.

6.2 Modeling Wage Dynamics in the Panel Study of Income Dynamics (PSID)

The Panel Study of Income Dynamics (PSID) is a long-running U.S. household survey that tracks individuals' income, employment, and demographics over time. Its repeated measurements create a natural clustered structure, with observations nested within individuals, making it a benchmark dataset for mixed-effects modeling. This case study applies GBMixed to the PSID data with preprocessing and model details described in Appendix D.

We model the log of wage as a function of education, experience, occupation, industry, gender, union status, and regional indicators, capturing the main determinants of earnings. Two groups of models are considered: the first uses the standard covariates as recorded in the raw data, while the second incorporates a decomposition of experience, informed by the diagnostic findings from the first stage.

We begin by fitting models using the untransformed covariates. Ordinary least squares establishes a linear benchmark, followed by nonparametric ensemble methods, Random Forest and XGBoost, which model nonlinear effects but do not account for repeated observations within individuals. These non-clustered models achieve moderate predictive accuracy, with test MSEs on the log-wage scale of 0.1386 and 0.1517, respectively (Table 6).

To account for the within-subject correlation, we next apply a linear mixed-effects model with random intercepts for individuals, representing differences in baseline wage levels. The model fits the data exceptionally well. Its large estimated within-subject correlation (0.516) confirms that a substantial portion of wage variation arises from stable individual effects, reducing the test MSE from 0.5809 (fixed

Table 6: Model comparison for PSID wage data. Test MSE is reported for fixed effects and for BLUPs (log-wage scale). Models marked * include random intercepts; ** include random intercepts and slopes.

Model	AIC	BIC	Test MSE (Fixed Only)	Test MSE (BLUPs)
Standard Covariates				
OLS	—	—	0.1933	—
RF	—	—	0.1386	—
XGB	—	—	0.1517	—
LMER*	265.71	349.68	0.5809	0.0395
GBMixed (MARS)*	—	—	0.2042	0.0810
GBoost (OLS/Tree)*	—	—	0.9413	0.0347
EXP Decomposition				
OLS	—	—	0.1057	—
RF	—	—	0.0750	—
XGB	—	—	0.0721	—
LMER**	−1181.56	−1079.59	0.1137	0.0325
GBMixed (MARS)**	—	—	0.1740	0.0321

effects only) to 0.0395 when including random effects (BLUPs).

GBMixed reproduces the linear mixed-effects structure when fitted with linear base learners, confirming equivalence to LMER. Extending GBMixed to a nonparametric mean function with MARS does not yield any improvement in BLUP accuracy (0.0810) likely because nonlinear mean terms absorb the variance previously attributed to random intercepts. Further analysis shows that attempts to flexibly model the mean function with nonparametric base learners produces similar results, reducing the random effects variance resulting in improved predictions with fixed effects only, at the expense of BLUP accuracy.

Given the importance of the random effects variance, we apply a GBoost model with a linear mean component and a nonparametric (tree-based) random-effect variance model which improves BLUP accuracy (0.0347) and reveals substantial heterogeneity in random intercepts. Variable importance (Table 10) identifies the experience covariate as the dominant driver with close to 50% of all the splits. Partial-dependence plots (Figure 9) reveal a U-shaped pattern of heterogeneity. This demonstrates that wage trajectories are most stable across time in the early and late career stages, with much more variation in the middle window.

Subject-specific wage trajectories (Figure 10), support this variation in both intercepts and slopes across individuals. To capture these patterns, experience was decomposed into two orthogonal components, between-subject and within-subject variation. The between-subject component (`EXP_between`) represents each individual’s mean experience across all observations, capturing long-term career differences. The within-subject component (`EXP_within`) captures deviations from that mean over time, representing short-term experience within the study period.

Models incorporating this decomposition improve predictive accuracy markedly. Under the expanded specification, LMER with random intercepts and a random slope for `EXP_within` shows substantial

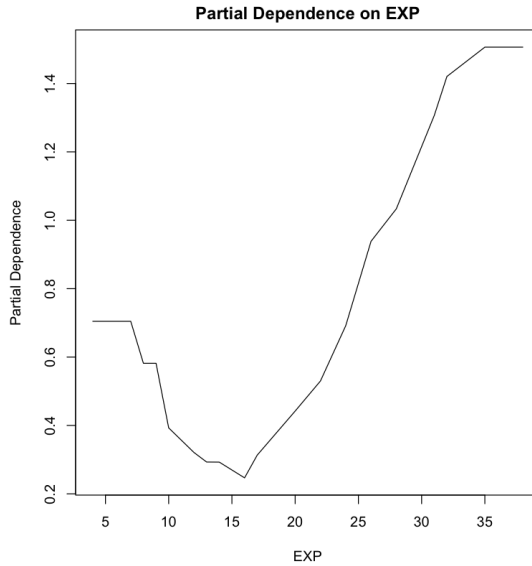


Figure 9: Partial dependence of random-effect variance on experience.

gains: AIC and BIC decrease by over 1000, and the test MSE (BLUPs) falls to 0.0325. GBMixed (with MARS for mean estimation) applied to the same structure achieves comparable accuracy, with a slight improvement over LMER. Examination of the partial dependence plots indicates that the leading predictors remain approximately linear, with only mild curvature in `WKS` and `EXP_between`, resulting in marginal gains in prediction performance.

This case study illustrates how GBMixed detects and models heterogeneity in random effects variance, leading to improved predictive performance and clearer interpretation of individual-level variation. By combining the interpretability of linear mixed models with the flexibility of boosting, GBMixed identifies when clustered structure should adapt.

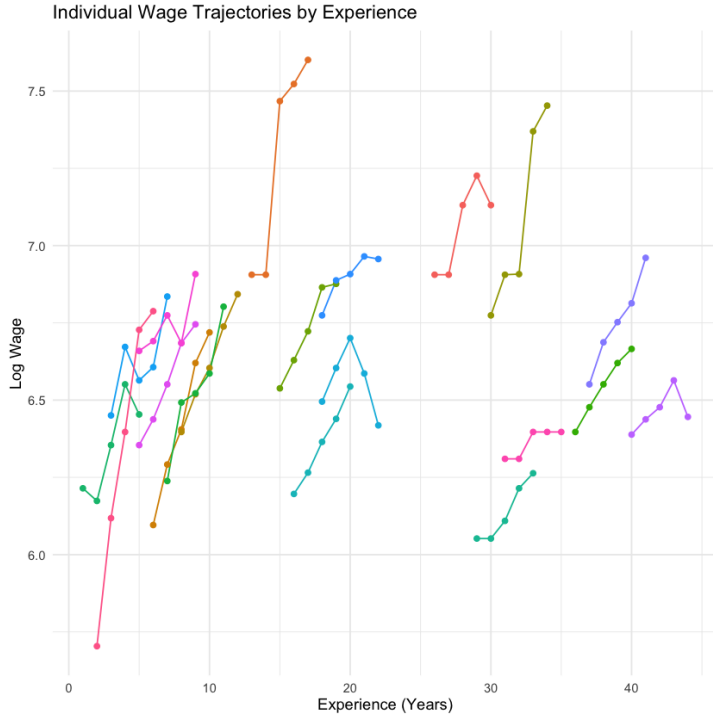


Figure 10: Individual wage trajectories by experience for a random sample of subjects.

7 Discussion and Future Work

7.1 Discussion

We demonstrated that Gradient Boosted Mixed Models can be applied to clustered data, combining the inferential strengths and uncertainty estimation of linear mixed models with the flexibility of modern machine learning through gradient boosting. The key contribution lies in the ability to jointly estimate mean and variance components using likelihood-based gradients, which results in high-performance mean prediction, well-calibrated prediction intervals, and reliable variance decomposition. The approach also allows variance to depend on covariates at both the group and observation level, uncovering patterns of heterogeneity that would otherwise remain hidden. At the same time, the method reconciles with linear mixed-effects models and standard gradient boosting machines, ensuring interpretability and familiarity with established approaches, when required. This combination of flexibility while maintaining statistical properties makes GBMixed well suited to applications in precision medicine, supply chain optimization and risk-reward decision optimization.

Despite these strengths, there are limitations. The algorithm is computationally more demanding than standard linear mixed models and many machine learning algorithms, particularly when applied to large datasets or complex random effect structures. It is typically slower than comparable approaches such as XGBoost because gradients for the mean, random effects, and residual variance components are modeled in parallel at each iteration.

As with other boosting methods, model performance depends on tuning parameters such as learning rates, tree depth, and stopping criteria, which may introduce sensitivity if not carefully calibrated. Finally, the current implementation focuses on Gaussian responses; extensions to generalized outcomes and broader distributional families are under development but not yet fully established.

The implications of this work are broad. The framework bridges the gap between statistics and machine learning, allowing for many applications of statistical inference and downstream optimization or decision making to be incorporated into machine learning algorithms. For example, this creates opportunities for more reliable uncertainty quantification in high-dimensional or nonlinear settings where traditional models struggle. The ability to detect heterogeneous treatment effects and covariate-dependent variance structures has direct value for applied domains such as clinical trials, policy evaluation, and financial pricing, where group-specific differences (patient or asset) are often masked under homogeneous assumptions. More generally, the framework highlights a path forward for statistical learning methods that retain interpretability and inference while expanding the scope of problems they can address.

7.2 Future Work

Future work will extend the algorithm to exponential family outcomes which appear feasible in the framework, with adjustments such as gradient approximations expected in some cases. This will broaden applicability to classification, count, and other outcome types while maintaining inferential validity.

Beyond the current focus on single-level clustered data, future research will explore the modeling of full hierarchical structures. This will enable the algorithm to capture dependency structures spanning more than one level of hierarchy and accommodate cross-classified random effects. Extensions will also investigate alternative variance structures, including spatial correlation models, allowing covariance components to depend on spatial distance.

Although the approach currently uses fixed learning rates, the framework allows these to be adjusted during training in response to model feedback. Such adaptive learning strategies could improve efficiency and stability by focusing updates where they are most valuable.

Ongoing software development will focus on improving runtime efficiency and scalability as well as expanding capabilities to include alternative base learners. There is also opportunity to include cross validation approaches for hyperparameter tuning. Together, these enhancements will broaden the flexibility of the framework while improving its practicality for applied research.

7.3 Concluding Remarks

The GBMixed algorithm represents a significant step in bringing together statistical and machine learning approaches under a single, likelihood-based boosting framework. By jointly modeling mean and variance components, it captures complex models, clustered data, and heterogeneous structures, while

maintaining accuracy, interpretability and inferential validity. The framework's modular software design opens opportunities for both theoretical development and practical deployment across diverse domains. A research-only implementation of the GBMixed framework is available upon request for selected academic or applied evaluation projects.

Acknowledgements

This research was conducted as part of a doctoral program at the Australian National University. The core methodology described in this paper is the subject of Australian Provisional Patent Application No. 2025902733, filed by the first author.

References

Breiman, L., Friedman, J.H., Olshen, R., and Stone, C. (1984). *Classification and Regression Trees*. Wadsworth, Belmont, CA.

Breiman, L. (2001). Random forests. *Machine Learning*, **45**(1), 5–32.

Bühlmann, P. and Yu, B. (2003). Boosting with the L_2 loss: Regression and classification. *Journal of the American Statistical Association*, **98**(462), 324–339. Taylor & Francis.

Bühlmann, P., and Hothorn, T. (2007). *Boosting Algorithms: Regularization, Prediction and Model Fitting*. Statistical Science, **22**(4), 477–505.

Chen, T., and Guestrin, C. (2016). *XGBoost: A Scalable Tree Boosting System*. In Proceedings of the 22nd ACM SIGKDD International Conference on Knowledge Discovery and Data Mining (pp. 785–794). ACM.

Chernozhukov, V., Chetverikov, D., Demirer, M., Duflo, E., Hansen, C., Newey, W., and Robins, J. (2018). Double/debiased machine learning for treatment and structural parameters. *The Econometrics Journal*, **21**(1), C1–C68. doi:10.1111/ectj.12097.

Cornwell, C., and Rupert, P. (1988). Efficient estimation with panel data: An empirical comparison of instrumental variables estimators. *Journal of Applied Econometrics*, **3**(2), 149–155.

Duan, T., Avati, A., Ding, D., Thai, K.K., Basu, S., Ng, A., and Schuler, A. (2019). *NGBoost: Natural Gradient Boosting for Probabilistic Prediction*. Stanford Machine Learning Group.

Fleming, T. R., and Harrington, D. P. (1991). *Counting Processes and Survival Analysis*. Wiley Series in Probability and Mathematical Statistics. John Wiley & Sons, New York.

Friedman, J. H. (1991). Multivariate Adaptive Regression Splines. *The Annals of Statistics*, 19(1), 1–67. <https://doi.org/10.1214/aos/1176347963>.

Friedman, J.H. (2001). *Greedy Function Approximation: A Gradient Boosting Machine*. Annals of Statistics 29(5):1189-1232.

Gu, C., and Ma, P. (2005). *Generalized Nonparametric Mixed-Effect Models: Computation and Smoothing Parameter Selection*. Journal of Computational and Graphical Statistics, 14(2), 485–504.

Henderson, C. R. (1950). *Estimation of Genetic Parameters*. Annals of Mathematical Statistics, 21, 309-310.

Holland, P. W. (1986). Statistics and causal inference. *Journal of the American Statistical Association*, 81(396), 945–960.

Karcher, P. and Wang, Y. (2001). *Generalized Nonparametric Mixed Effects Models*. Journal of Computational and Graphical Statistics, 10, 641–655.

Knieper, L., Hothorn, T., Bergherr, E., and Griesbach, C. (2025). Gradient boosting for generalized additive mixed models. *Statistics and Computing*, 35:84. doi:10.1007/s11222-025-10612-y.

Lindstrom, M. J., and Bates, D. M. (1990). *Nonlinear Mixed Effects Models for Repeated Measures Data*. Biometrics 46:673–687.

Mason, L., Baxter, J., Bartlett, P. L., and Frean, M. (1999). Functional gradient techniques for combining hypotheses. *Advances in Neural Information Processing Systems*, 12, 221–246.

McCulloch, C. E., and Searle, S. R. (2001). *Generalized, Linear, and Mixed Models*. Wiley Series in Probability and Statistics. Wiley-Interscience.

Petersen, K. B., and Pedersen, M. S. (2012). *The Matrix Cookbook*. Technical University of Denmark. Available online: <https://www.math.uwaterloo.ca/~hwolkowi/matrixcookbook.pdf>

Rigby, R. A., and D. M. Stasinopoulos (2005). Generalized additive models for location, scale and shape (with discussion). *Journal of the Royal Statistical Society: Series C (Applied Statistics)*, 54(3), 507–554. doi:10.1111/j.1467-9876.2005.00510.x.

Rubin, D. B. (1974). Estimating causal effects of treatments in randomized and nonrandomized studies. *Journal of Educational Psychology*, 66(5), 688–701.

Ruckstuhl, A. F., Welsh, A. H., and Carroll, R. J. (2000). *Nonparametric Function Estimation of the Relationship Between Two Repeatedly Measured Variables*. Statistica Sinica, 10(1), 51–71.

Tan, Y. V., and Roy, J. (2019). Bayesian additive regression trees and the General BART model. *Statistics in Medicine*, 38(25), 5048–5069. <https://doi.org/10.1002/sim.8347>

Tran, M.-N., Nguyen, N., Nott, D., and Kohn, R. (2019). Bayesian Deep Net GLM and GLMM. *Journal of Computational and Graphical Statistics*, 29(1), 97–113. <https://doi.org/10.1080/10618600.2019.1637747>

Searle, S. R., Casella, G., and McCulloch, C. E. (2006). *Variance Components*. Wiley.

Sigrist, F. (2022). Gaussian process boosting. *Journal of Machine Learning Research*, 23(40), 1–67.

Stock, J. H., and Watson, M. W. (2007). *Introduction to Econometrics* (2nd ed.). Boston: Pearson.

Wager, S., and Athey, S. (2017). *Estimation and Inference of Heterogeneous Treatment Effects using Random Forests*. *Journal of the American Statistical Association*, 113(523), 1228–1242.

Zhang, T. and Yu, B. (2005). Boosting with early stopping: Convergence and consistency. *The Annals of Statistics*, 33(4), 1538–1579. Institute of Mathematical Statistics.

Appendix A: Gradient Derivations for the Gaussian Case

This appendix presents the core gradient derivations used for the Gaussian response case. Our objective is to provide a transparent breakdown of the gradients of the log-likelihood with respect to the mean vector and variance components. These derivations are based on the multivariate normal marginal likelihood, which arises naturally from integrating out the random effects in a mixed model. The presentation proceeds in two parts. We first derive general results for a multivariate Gaussian model with arbitrary mean vector μ and covariance matrix Σ , establishing the foundational gradients. We then extend these results to the parameterization $\Sigma = \mathbf{Z}\mathbf{G}\mathbf{Z}^\top + \mathbf{R}$, which reflects the variance decomposition used in GBMixed. In this setting, we derive expressions for the gradients with respect to the fixed effects, the random effect covariance matrix \mathbf{G} , and the residual variance matrix \mathbf{R} , including scalar and heteroscedastic cases. For clarity, all gradients are defined at the group level; however, to simplify notation we omit the subscript i throughout the derivations.

A.1 Mixed Effects Model and Marginal Gaussian Form

We consider the general mixed effects model introduced in Section 3. In the following sections, we derive the analytic gradients of the log-likelihood with respect to μ and Σ , providing the basis for gradient-based estimation of both mean and variance components within the GBMixed framework.

A.2 Log-Likelihood and Gradients with Respect to μ and Σ

The multivariate Gaussian log-likelihood for a specific group with response vector \mathbf{y} is

$$\ell(\boldsymbol{\mu}, \boldsymbol{\Sigma}; \mathbf{y}) = -\frac{n}{2} \log(2\pi) - \frac{1}{2} \log |\boldsymbol{\Sigma}| - \frac{1}{2} (\mathbf{y} - \boldsymbol{\mu})^\top \boldsymbol{\Sigma}^{-1} (\mathbf{y} - \boldsymbol{\mu}).$$

We now derive the gradients of this expression with respect to the mean vector $\boldsymbol{\mu}$ and the covariance matrix $\boldsymbol{\Sigma}$, using standard results from the Matrix Cookbook (Petersen and Pedersen, 2012).

A.2.1 Gradient with Respect to μ

We begin by isolating the quadratic term:

$$f(\boldsymbol{\mu}) = (\mathbf{y} - \boldsymbol{\mu})^\top \boldsymbol{\Sigma}^{-1} (\mathbf{y} - \boldsymbol{\mu}).$$

Expanding the quadratic form:

$$f(\boldsymbol{\mu}) = \mathbf{y}^\top \boldsymbol{\Sigma}^{-1} \mathbf{y} - 2\boldsymbol{\mu}^\top \boldsymbol{\Sigma}^{-1} \mathbf{y} + \boldsymbol{\mu}^\top \boldsymbol{\Sigma}^{-1} \boldsymbol{\mu}.$$

Differentiating with respect to $\boldsymbol{\mu}$:

$$\frac{\partial f}{\partial \boldsymbol{\mu}} = -2\boldsymbol{\Sigma}^{-1} \mathbf{y} + 2\boldsymbol{\Sigma}^{-1} \boldsymbol{\mu} = 2\boldsymbol{\Sigma}^{-1} (\boldsymbol{\mu} - \mathbf{y}).$$

Hence, the gradient of the log-likelihood is:

$$\frac{\partial \ell}{\partial \boldsymbol{\mu}} = \boldsymbol{\Sigma}^{-1} (\mathbf{y} - \boldsymbol{\mu})$$

(A.1)

A.2.2 Gradient with Respect to Σ

We now differentiate Equation (A.4) with respect to $\boldsymbol{\Sigma}$. Let $\mathbf{s} = \mathbf{y} - \boldsymbol{\mu}$ denote the residual vector.

The derivative of the log-determinant is:

$$\frac{\partial}{\partial \boldsymbol{\Sigma}} \log |\boldsymbol{\Sigma}| = \boldsymbol{\Sigma}^{-1}.$$

The quadratic term can be rewritten using the trace identity:

$$\mathbf{s}^\top \boldsymbol{\Sigma}^{-1} \mathbf{s} = \text{Tr} (\boldsymbol{\Sigma}^{-1} \mathbf{s} \mathbf{s}^\top).$$

Differentiating this term:

$$\frac{\partial}{\partial \boldsymbol{\Sigma}} \text{Tr} (\boldsymbol{\Sigma}^{-1} \mathbf{s} \mathbf{s}^\top) = -\boldsymbol{\Sigma}^{-1} \mathbf{s} \mathbf{s}^\top \boldsymbol{\Sigma}^{-1}.$$

Combining both parts, the full gradient of the log-likelihood with respect to Σ is:

$$\boxed{\frac{\partial \ell}{\partial \Sigma} = -\frac{1}{2} (\Sigma^{-1} - \Sigma^{-1} s s^\top \Sigma^{-1})} \quad (\text{A.2})$$

This expression underlies all subsequent derivations for the parameterized forms of Σ .

A.3 Gradient Functions for \mathbf{G} and \mathbf{R} Parameterization

We now derive the score functions for the marginal Gaussian log-likelihood under the general parameterization

$$\Sigma = \mathbf{Z} \mathbf{G} \mathbf{Z}^\top + \mathbf{R},$$

where $\mathbf{G} \in \mathbb{R}^{q \times q}$ denotes the covariance matrix of the random effects, and $\mathbf{R} \in \mathbb{R}^{n_i}$ denotes the residual covariance matrix. This formulation accommodates arbitrary random effects structures, including correlated random slopes, unbalanced group sizes, and heteroscedastic residuals.

We assume the same marginal distribution and log-likelihood structure, with mean vector $\mu = f(\mathbf{X})$, residual vector $s = \mathbf{y} - \mu$, and

$$\ell(\mu, \Sigma; \mathbf{y}) = -\frac{1}{2} \log |\Sigma| - \frac{1}{2} s^\top \Sigma^{-1} s + \text{constant}.$$

The gradient with respect to the mean vector μ remains unchanged and is given by the general result in Equation (A.1).

A.3.1 Gradient with Respect to \mathbf{G}

To compute the score function with respect to the random effects covariance matrix \mathbf{G} , we begin by differentiating the marginal log-likelihood starting with the derivative of Σ with respect to \mathbf{G} which is given by

$$d\Sigma = \mathbf{Z} (d\mathbf{G}) \mathbf{Z}^\top.$$

The gradient of the log-determinant term is

$$\frac{\partial}{\partial \mathbf{G}} \log |\Sigma| = \text{Tr} \left(\Sigma^{-1} \frac{\partial \Sigma}{\partial \mathbf{G}} \right) = \Sigma^{-1} : \frac{\partial \Sigma}{\partial \mathbf{G}},$$

where \cdot denotes the Frobenius inner product, defined as $\mathbf{A} : \mathbf{B} = \text{Tr}(\mathbf{A}^\top \mathbf{B})$. Using the identity $\Sigma^{-1} : (\mathbf{Z} \otimes \mathbf{Z}) = \mathbf{Z}^\top \Sigma^{-1} \mathbf{Z}$, we simplify to

$$\Sigma^{-1} : \frac{\partial \Sigma}{\partial \mathbf{G}} = \mathbf{Z}^\top \Sigma^{-1} \mathbf{Z}.$$

The derivative of the quadratic term is given by the identity

$$\frac{\partial}{\partial \mathbf{X}} (\tilde{\mathbf{x}}^\top \mathbf{X}^{-1} \tilde{\mathbf{x}}) = -\mathbf{X}^{-1} \tilde{\mathbf{x}} \tilde{\mathbf{x}}^\top \mathbf{X}^{-1},$$

which implies

$$\frac{\partial}{\partial \mathbf{G}} (\mathbf{s}^\top \boldsymbol{\Sigma}^{-1} \mathbf{s}) = -\mathbf{Z}^\top \boldsymbol{\Sigma}^{-1} \mathbf{s} \mathbf{s}^\top \boldsymbol{\Sigma}^{-1} \mathbf{Z}.$$

Combining the two components yields the gradient of the log-likelihood with respect to \mathbf{G} :

$$\boxed{\frac{\partial \ell}{\partial \mathbf{G}} = -\frac{1}{2} (\mathbf{Z}^\top \boldsymbol{\Sigma}^{-1} \mathbf{Z} - \mathbf{Z}^\top \boldsymbol{\Sigma}^{-1} \mathbf{s} \mathbf{s}^\top \boldsymbol{\Sigma}^{-1} \mathbf{Z})} \quad (\text{A.3})$$

This expression can be simplified further for implementation by letting $\mathbf{r} = \mathbf{Z}^\top \boldsymbol{\Sigma}^{-1} \mathbf{s}$, in which case the second term becomes $\mathbf{r} \mathbf{r}^\top$, and we obtain:

$$\frac{\partial \ell}{\partial \mathbf{G}} = -\frac{1}{2} (\mathbf{Z}^\top \boldsymbol{\Sigma}^{-1} \mathbf{Z} - \mathbf{r} \mathbf{r}^\top).$$

A.3.2 Cholesky Gradient Transformation to \mathbf{G}

We apply the chain rule for the Cholesky gradient transformation to ensure positive definiteness;

$$\frac{\partial \ell}{\partial L_{ij}} = \text{Tr} \left[\left(\frac{\partial \ell}{\partial \mathbf{G}} \right)^\top \frac{\partial \mathbf{G}}{\partial L_{ij}} \right]$$

This form expresses how changes in \mathbf{L} affect ℓ via its dependence on $\mathbf{G} = \mathbf{L} \mathbf{L}^\top$.

To proceed, we compute the differential of \mathbf{G} using the product rule:

$$d\mathbf{G} = (d\mathbf{L}) \mathbf{L}^\top + \mathbf{L} (d\mathbf{L})^\top$$

Substituting into the trace form:

$$d\ell = \text{Tr} \left(\left(\frac{\partial \ell}{\partial \mathbf{G}} \right)^\top ((d\mathbf{L}) \mathbf{L}^\top + \mathbf{L} (d\mathbf{L})^\top) \right)$$

Use the cyclic property of the trace and transpose symmetry of $\frac{\partial \ell}{\partial \mathbf{G}}$ to isolate $d\mathbf{L}$:

$$d\ell = 2 \text{Tr} \left(\left(\frac{\partial \ell}{\partial \mathbf{G}} \mathbf{L} \right)^\top d\mathbf{L} \right)$$

Comparing with the general identity for differentials of scalar functions:

$$d\ell = \text{Tr} \left(\left(\frac{\partial \ell}{\partial \mathbf{L}} \right)^\top d\mathbf{L} \right)$$

we obtain the final expression for the gradient:

$$\boxed{\frac{\partial \ell}{\partial \mathbf{L}} = 2 \frac{\partial \ell}{\partial \mathbf{G}} \mathbf{L}} \quad (\text{A.4})$$

A.3.3 Gradient with Respect to \mathbf{R}

We now derive the score function with respect to the residual covariance matrix \mathbf{R} . This gradient applies to general heteroscedastic or correlated residual structures. Recall that the marginal covariance matrix is given by $\Sigma = \mathbf{Z}\mathbf{G}\mathbf{Z}^\top + \mathbf{R}$. The derivative of Σ with respect to \mathbf{R} is simply

$$d\Sigma = d\mathbf{R}.$$

The gradient of the log-determinant term is

$$\frac{\partial}{\partial \mathbf{R}} \log |\Sigma| = \Sigma^{-1}.$$

The derivative of the quadratic term follows the identity

$$\frac{\partial}{\partial \mathbf{X}} \left(\tilde{\mathbf{x}}^\top \mathbf{X}^{-1} \tilde{\mathbf{x}} \right) = -\mathbf{X}^{-1} \tilde{\mathbf{x}} \tilde{\mathbf{x}}^\top \mathbf{X}^{-1},$$

which yields

$$\frac{\partial}{\partial \mathbf{R}} (s^\top \Sigma^{-1} s) = -\Sigma^{-1} s s^\top \Sigma^{-1}.$$

Combining the two components, the gradient of the log-likelihood with respect to the residual covariance matrix \mathbf{R} is

$$\boxed{\frac{\partial \ell}{\partial \mathbf{R}} = -\frac{1}{2} (\Sigma^{-1} - \Sigma^{-1} s s^\top \Sigma^{-1})}. \quad (\text{A.5})$$

This expression holds for any symmetric residual covariance matrix $\mathbf{R} \in \mathbb{R}^{n \times n}$, including the general correlated case.

Simplification for Diagonal Residual Structure. When $\mathbf{R} = \text{diag}(\sigma_1^2, \dots, \sigma_n^2)$, the residual variance is heterogeneous across observations. If all $\sigma_i^2 = \sigma^2$, this further simplifies to the homoscedastic case $\mathbf{R} = \sigma^2 \mathbf{I}_n$. In the heterogeneous case, the gradient with respect to each diagonal element σ^2 can be extracted from the general matrix gradient by evaluating the i -th diagonal entry.

The derivative of the log-determinant term becomes:

$$[\Sigma^{-1}]_{ii}.$$

The derivative of the quadratic term becomes:

$$[\boldsymbol{\Sigma}^{-1} \mathbf{s} \mathbf{s}^\top \boldsymbol{\Sigma}^{-1}]_{ii} = ([\boldsymbol{\Sigma}^{-1} \mathbf{s}]_i)^2.$$

The gradient with respect to each individual diagonal variance component σ^2 in the heteroscedastic case is given by:

$$\frac{\partial \ell}{\partial \sigma^2} = -\frac{1}{2} \left((\boldsymbol{\Sigma}^{-1})_{ii} - [\boldsymbol{\Sigma}^{-1} \mathbf{s}]_i^2 \right) \quad \text{for } i = 1, \dots, n.$$

This expression holds whether the residual variances are heterogeneous or constant across observations.

In the homoscedastic case where $\mathbf{R} = \sigma^2 \mathbf{I}_n$, the log-likelihood gradient simplifies to:

$$\boxed{\frac{d\ell}{d\sigma^2} = -\frac{1}{2} \left(\text{Tr}(\boldsymbol{\Sigma}^{-1}) - \|\boldsymbol{\Sigma}^{-1} \mathbf{s}\|^2 \right).} \quad (\text{A.6})$$

Appendix B: Simulation Experiments

This appendix details the simulation designs, data-generating processes (DGPs), model hyperparameters, and worked examples used to evaluate performance, calibration, and variance recovery.

Coverage is assessed in two different ways. For GBMixed, coverage is evaluated by comparing the 90% prediction interval for the treatment contrast to the true potential outcome difference $Y_{ij}(1) - Y_{ij}(0)$:

$$Y_{ij}(1) - Y_{ij}(0) \in \left[\hat{\tau}(\mathbf{x}_{ij}) \pm \Phi^{-1}(1 - \alpha/2) \sqrt{\text{Var}(Y_{ij}(1) - Y_{ij}(0) \mid \mathbf{x}_{ij})} \right],$$

where $\hat{\tau}(\mathbf{x}_{ij})$ is the estimated CATE from the GBMixed model.

For OLS, LMER and CF, coverage is assessed as the proportion of simulated observations where the true treatment effect lies within the estimated interval. This involves checking whether the simulated treatment effect $\tau(\mathbf{x}_{ij})$ falls inside the estimated confidence interval centered at the CATE estimate $\hat{\tau}(\mathbf{x}_{ij})$ with width determined by its estimated standard error $\hat{\sigma}_\tau$:

$$\tau(\mathbf{x}_{ij}) \in \left[\hat{\tau}(\mathbf{x}_{ij}) \pm \Phi^{-1}(1 - \alpha/2) \hat{\sigma}_\tau(\mathbf{x}_{ij}) \right].$$

B.1 Experiment A: Nonlinear Matched-Pairs Model with Heterogeneous Treatment Effects

This experiment introduces the core simulation framework used to evaluate GBMixed. The design combines nonlinear covariate relationships, mixed predictor types, heterogeneous treatment effects, and within-group dependence through random effects. It is intended to assess how well GBMixed estimates

conditional treatment effects and variance components in high-dimensional situations, with non-Gaussian covariates where random intercepts are present. The scenario reflects a realistic test for examining predictive accuracy, calibration of uncertainty intervals, and the robustness of variance estimation under a complex clustered structure.

The experiment is run across 100 independent simulations and results are aggregated unless otherwise stated.

B.1.1 Experimental Design

The simulation generates $n = 10,000$ observations nested within matched pairs, with $p = 300$ covariates. Sixty percent of the data are used for model training and the remaining forty percent for validation and held-out test evaluation. Covariates are sampled from a mixture of continuous, binary, and count distributions to reflect heterogeneous data sources:

$$x_1 \sim \mathcal{N}(0, 1), \quad x_2 \sim U(0, 2), \quad x_3 \sim \text{Bernoulli}(0.5), \quad x_4 \sim \text{Poisson}(1.5), \quad x_{5:300} \sim \mathcal{N}(0, 1).$$

Treatment is randomly assigned within each matched pair, $w_{ij} \in \{0, 1\}$, ensuring unconfounded assignment while maintaining group-level correlation through random intercepts.

The response model is defined as

$$y_{ij} = \alpha_i + m(x_{ij}) + \tau(x_{ij}) w_{ij} + \epsilon_{ij}, \quad \alpha_i \sim \mathcal{N}(0, \sigma_\alpha^2), \quad \epsilon_{ij} \sim \mathcal{N}(0, \sigma_\epsilon^2),$$

with $\sigma_\alpha^2 = 2.25$ and $\sigma_\epsilon^2 = 0.47$. This formulation induces both between-group and within-group variability, providing a rigorous setting for evaluating variance component recovery and conditional treatment effect estimation.

The nonlinear baseline function introduces additive, interaction, and logarithmic terms:

$$m(x_{ij}) = 0.5 \sin(x_{ij,1}) + 0.1 x_{ij,2}^2 + 0.1 x_{ij,3} x_{ij,4} + 0.3 \log(x_{ij,4} + 1) x_{ij,5} + x_{ij,1} x_{ij,5}.$$

Heterogeneous treatment effects are generated using a smooth surface based on sigmoids:

$$\tau(x_{ij}) = \varsigma(x_{ij,6}) \varsigma(x_{ij,7}), \quad \varsigma(x) = \frac{1}{1 + e^{-20(x-1/3)}}.$$

B.1.3 GBMixed Implementation

The GBMixed model is implemented to jointly estimate the nonlinear mean function and variance components while accounting for group-level random effects. All models use tree base learners with shallow depth to balance flexibility and interpretability.

The model is trained for 500 boosting iterations with learning rates of 0.03 for both the mean and variance updates. Subsampling is performed at 20% of observations and 70% of predictors per iteration. Shallow regression trees (maximum depth = 3, minimum parent size = 10, minimum child size = 5) are used as base learners for the mean component. Random intercepts are included and updated via constant mean updates, capturing within-group correlation. Random effects variance components are updated using a Cholesky parameterization to preserve positive definiteness. Early stopping is disabled to ensure a consistent number of iterations across replications.

The treatment indicator variable is always included in the sampled feature set to ensure stability in heterogeneous treatment effect estimation and comparability with CF. In order to compare the other approaches on an equal footing, the RF algorithm is adjusted so that the treatment effect is forced into the consideration set for each tree with the `always.split.variables` option. XGB does not support an `always.split.variables` option. Instead feature weighting was tested by assigning a high weight (1000) to the treatment indicator and unit weights to other covariates; however, the resulting CATE MSE improved only marginally, so the standard unweighted approach was retained for all reported experiments. No such option exists for other comparison approaches.

These settings were selected to balance model flexibility, computational efficiency, and stability of variance estimation in high-dimensional clustered data.

B.1.4 Results

Figure 11 presents the convergence analysis for a single experiment / simulation, illustrating the model’s stability during training. The log-likelihood and MSE show a smooth, steady convergence pattern. The estimated random effect component follows an interesting stabilization pattern initially decreasing, then increasing, before leveling off around 300 trees / iterations. Residual variance also follows a smooth convergence pattern. These findings indicate that GBMixed successfully converges.

Table 2 reports overall performance across methods. GBMixed achieves the lowest CATE mean-squared error and coverage close to the nominal 90%, clearly outperforming all comparators. OLS and LMER fail to capture nonlinear treatment heterogeneity, while tree-based learners (particularly RF) show notable improvement in modeling nonlinear relationships but still exhibit weaker calibration. Causal Forest (CF) performs poorly on accuracy and also substantially underestimates coverage, indicating poorly calibrated uncertainty.

These findings demonstrate that when applied to high dimensional non-linear data, GBMixed effectively captures treatment effect heterogeneity while maintaining reliable uncertainty quantification.

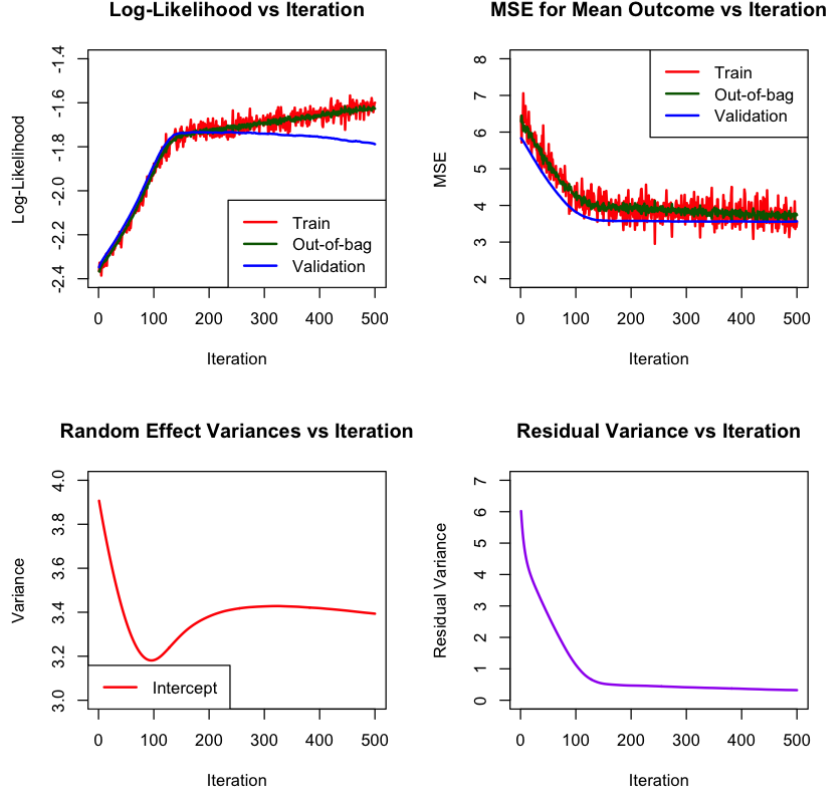


Figure 11: Convergence Analysis of GBMixed in Experiment A

B.2 Experiment B: Covariate-Dependent Residual Heteroscedasticity

B.2.1 Experimental Design

This experiment extends the nonlinear matched-pairs framework of Experiment A to evaluate model performance under covariate-dependent residual variance. The goal is to test whether GBMixed (and its residual variance extension, RBoost) can accurately estimate both the CATE and the heteroscedastic error structure $R(\mathbf{x}_{ij})$. The experiment is again run across 100 independent simulations and results are aggregated unless otherwise stated.

B.2.2 Model Specification

Covariates are simulated as:

$$x_{1:30} \sim U(0, 1),$$

with $n = 10,000$ total observations and $p = 30$ predictors. Sixty percent of observations are used for training and forty percent for validation and held-out testing.

The response model is defined as:

$$y_{ij} = \alpha_i + m(x_{ij}) + \tau(x_{ij})w_{ij} + \epsilon_{ij}, \quad \alpha_i \sim \mathcal{N}(0, \sigma_\alpha^2), \quad \epsilon_{ij} \sim \mathcal{N}(0, R(\mathbf{x}_{ij})),$$

where $w_{ij} \in \{0, 1\}$ denotes treatment assignment within matched pairs.

The baseline and treatment functions are defined as:

$$m(x_{ij}) = 2x_{ij,1} + 1, \quad \tau(x_{ij}) = \varsigma(x_{ij,1})\varsigma(x_{ij,2}), \quad \varsigma(x) = \frac{1}{1 + e^{-20(x-1/3)}}.$$

Residual variance varies systematically with covariates:

$$R(x_{ij}) = 0.3 + 0.4|x_{ij,2} - 0.5| + 0.4\mathbf{1}(x_{ij,5} \geq 0.5),$$

creating both continuous and discrete heteroscedasticity patterns that challenge models assuming constant variance.

The random intercept variance σ_α^2 is set to 0.25.

B.2.3 GBMixed Implementation

The implementation of GBMixed in Experiment B follows the same general procedure as in Experiment A, except that the model explicitly incorporates a covariate-dependent residual variance function through the RBoost extension. This enables joint estimation of the mean and variance components when residual variance is heteroscedastic.

The model is trained for 500 boosting iterations with learning rates of 0.01 for both the mean and variance updates. Subsampling is performed at 20% of observations and 70% of predictors per iteration. Shallow regression trees (maximum depth = 3, minimum parent size = 10, minimum child size = 5) are used as base learners for the mean component. Random intercepts are included and updated via constant mean updates, capturing within-group correlation.

Unlike Experiment A, the variance component is updated at each iteration via the RBoost learner, which models $R(\mathbf{x}_{ij})$ directly as a smooth function of covariates. The same base learner and hyperparameter settings are applied (shallow regression trees with maximum depth = 3, minimum parent size = 10, minimum child size = 5). This configuration allows the model to capture heteroscedasticity present in the data-generating process.

B.2.4 Results

Table 3 reports model performance under covariate-dependent residual heteroscedasticity. GBMixed attains the lowest CATE MSE (0.0047), substantially outperforming all other methods, and achieves coverage close to the nominal 90% target (88.3%). Linear models (OLS, LMER) cannot capture heteroscedastic residual variance and therefore provide only baseline accuracy with very low coverage. Both random forest and XGBoost degrade under this design, showing higher CATE error. Causal Forest attains moderate CATE accuracy but severely underestimates uncertainty, resulting in poor coverage.

In contrast, GBMixed performs consistently well, achieving the lowest error and reliable uncertainty quantification across both mean and variance components.

The R_{ij} MSE quantifies how accurately each method estimates the ground-truth covariate-dependent residual variance. GBMixed achieves the lowest R_{ij} MSE (0.0163) compared to LMER (0.0633), confirming its ability to recover the true heteroscedastic structure.

Figure 12 illustrates GBMixed’s ability to estimate heteroscedastic residual variance for a single simulation. The scatter plot compares the predicted residual variance against the true residual variance for test observations. GBMixed successfully captures the complex pattern of heteroscedasticity, showing two major clusters corresponding to the step function on x_5 and a gradual fanning pattern corresponding to the relationship with x_2 .

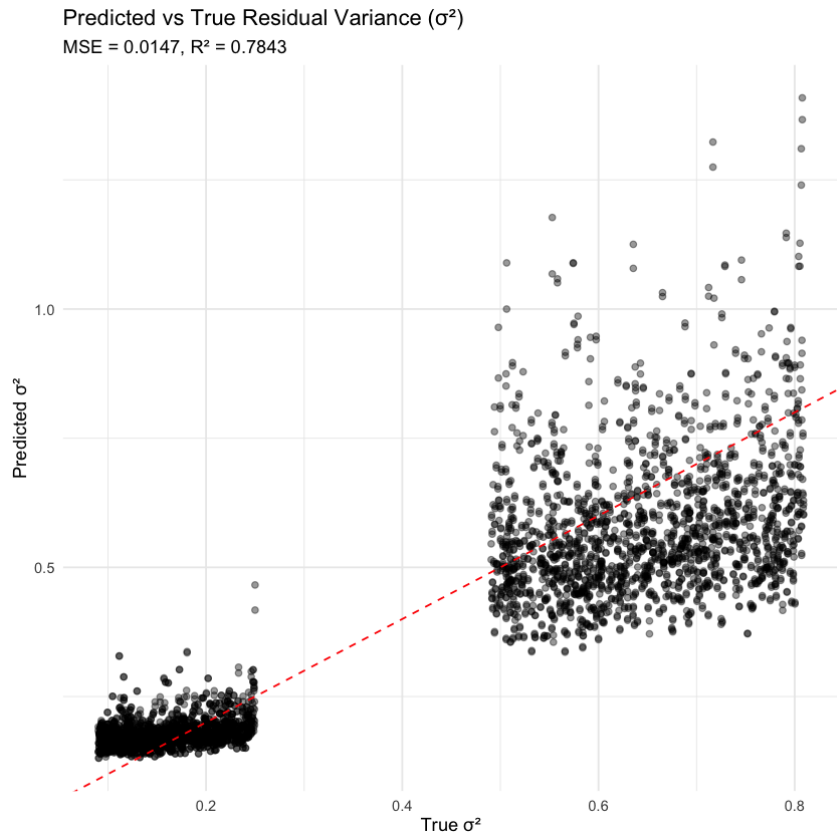


Figure 12: Predicted vs. True Residual Variance in Experiment B

The results from Experiment B highlight GBMixed’s ability to model heteroscedastic residual variance while maintaining high accuracy in treatment effect estimation. This capability is particularly valuable in settings where the error variance depends on covariates, a common scenario in real-world applications.

B.3 Experiment C: Heterogeneous Random Effect and Residual Variance

B.3.1 Experimental Design

Experiment C represents the most complex variance scenario, combining both heterogeneous random effects variance and heteroscedastic residual variance in a single model. This creates a challenging clustered structure where both between-group and within-group variance components vary systematically across the covariate space. The goal is to test whether GBMixed (with its extension, GRBoost) can accurately estimate the conditional treatment effect, the heteroscedastic residual error structure $R(\mathbf{x}_{ij})$, and the heterogeneous random effects error structure $G(\tilde{\mathbf{x}}_i)$. The experiment is again run across 100 independent simulations and results are aggregated unless otherwise stated.

B.3.2 Model Specification

This experiment extends the previous designs by introducing heterogeneity in both the random-effect and residual variances, creating covariate-dependent structures for G_i and R_{ij} .

Covariates are simulated as:

$$x_{1:30} \sim U(0, 1),$$

with $n = 10,000$ total observations and $p = 30$ predictors. Sixty percent of observations are used for model training and forty percent for validation and held-out testing.

The response model is defined as:

$$y_{ij} = \alpha_i + m(x_{ij}) + \tau(x_{ij}) w_{ij} + \epsilon_{ij}, \quad \alpha_i \sim \mathcal{N}(0, G(\tilde{\mathbf{x}}_i)), \quad \epsilon_{ij} \sim \mathcal{N}(0, R(\mathbf{x}_{ij})),$$

where $w_{ij} \in \{0, 1\}$ denotes treatment assignment within matched pairs.

The baseline and treatment functions are defined as:

$$m(x_{ij}) = 2x_{ij,1} + 1, \quad \tau(x_{ij}) = \varsigma(x_{ij,1}) \varsigma(x_{ij,2}), \quad \varsigma(x) = \frac{1}{1 + e^{-20(x-1/3)}}.$$

The variance components vary systematically with covariates:

$$R(\mathbf{x}_{ij}) = 0.4 + 0.4 |x_{ij,5} - 0.5|, \quad G(\tilde{\mathbf{x}}_i) = 0.5 + 1.5 |\tilde{x}_{i,3} - 0.5|.$$

B.3.3 GBMixed Implementation

GBMixed is implemented using the GRBoost configuration, which jointly models heterogeneity in both the random effects variance and residual variance through covariate-dependent functions. This formulation combines the GBoost and RBoost components within a single iterative boosting framework, allowing simultaneous updates of the mean and variance structures.

The model is trained for 500 boosting iterations with learning rates of 0.03 for both the mean and variance components. Subsampling is performed at 20% of observations and 70% of predictors per iteration. Updates are fit using shallow regression trees (maximum depth = 3, minimum parent size = 10, minimum child size = 5) as base learners, applied identically to all components — mean, random effects variance, and residual variance.

The random effects structure is specified using the formula $\sim 1 + \text{Group}$, capturing group-specific random intercepts. Both the group-level variance and residual variance are modeled as smooth functions of covariates using the same tree-based learner (shallow regression trees with maximum depth = 3, minimum parent size = 10, minimum child size = 5), enabling the model to recover complex variance patterns.

B.3.4 Results

Table 4 reports model performance under joint heterogeneity in both random-effect and residual variances. GBMixed (GRBoost) achieves the best overall performance across all metrics, with the lowest CATE MSE (0.0057) and near-nominal prediction interval coverage (89.3% vs. a 90% target). It also provides the most accurate estimation of both variance components, achieving the lowest R_{ij} MSE (0.0148) and G_i MSE (1.99), confirming its ability to jointly model complex cluster variability.

Linear models (OLS, LMER) perform poorly, with high CATE MSE and very low empirical coverage, as they do not provide heterogeneity in either treatment effect or variance component estimation. Random forest and XGBoost perform equally poor in CATE accuracy and do not recover group-level or residual variance patterns. Causal Forest attains reasonable CATE accuracy and coverage but does not capture the structured variance components. In contrast, GBMixed delivers both strong predictive accuracy and reliable uncertainty quantification, demonstrating its advantage in modeling nonlinear mixed-effect structures with covariate-dependent variance.

Table 7 demonstrates GBMixed’s ability to recover heterogeneous random effects variance in Experiment C for a single simulation. The experiment includes two distinct groups with different random effect standard deviations: 0.5 and 2.0.

The standard linear mixed-effects model estimates a single random effect standard deviation (1.45) for all groups, as it assumes homogeneous variance components.

Table 7: Group-Level Random Effect SDs: Predicted vs True vs LMER			
True SD	LMER Estimate	GBMixed Predicted	Mean
0.5	1.45	0.631	
2.0	1.45	1.933	

In contrast, GBMixed successfully captures the heterogeneity in random effects variance, providing group-specific estimates that track the true values much more closely (0.631 vs. true 0.5 for low-variance

groups, and 1.933 vs. true 2.0 for high-variance groups). While there is still some bias in the estimates, GBMixed clearly differentiates between the two variance groups and provides much more accurate estimates than LMER.

Table 8 reveals another critical aspect of GBMixed’s modeling capabilities in complex clustered data structures. In Experiment C, the residual standard deviations vary across observations based on covariates, with true values of 0.4 and 0.8 for different groups.

The standard linear mixed-effects model can only estimate a single residual standard deviation (0.622) for all observations, representing an average across the heterogeneous structure.

GBMixed, with its flexible boosting approach to variance component modeling, successfully captures this heteroscedasticity pattern, estimating group-specific residual standard deviations of 0.455 and 0.74, which closely track the true values.

Table 8: Residual SDs: Predicted vs True vs LMER

True SD	LMER Estimate	GBMixed Predicted Mean
0.4	0.622	0.455
0.8	0.622	0.740

The combination of accurately modeling both heterogeneous random effects and heteroscedastic residuals allows GBMixed to provide well-calibrated prediction intervals, resulting in its strong coverage performance. This demonstrates GBMixed’s unique advantage in uncertainty quantification for complex clustered data structures with multiple sources of heterogeneity.

Appendix C: Supplementary Materials for the PBC Application

C.1 Dataset Description

The primary biliary cirrhosis (PBC) dataset from the Mayo Clinic trial is a widely used benchmark in the survival and clinical modeling literature (Fleming and Harrington, 1991), sourced from the `mixAK` package as `PBCseq`. It contains longitudinal measurements on 312 patients (1945 observations in total) with advanced liver disease, including treatment assignment, demographic variables, and biochemical markers. The dataset is characterized by clustered structure due to repeated measures within subjects and heterogeneous disease progression across patients, making it a natural candidate for mixed model applications.

We model log-transformed serum glutamic oxaloacetic transaminase (SGOT/AST), a biomarker of liver inflammation, to evaluate the performance of GBMixed, which combines the flexibility of gradient boosting with the structured random effects of mixed models. Patients contributed between 1 and 27 visits each.

Missingness is substantial for some biomarkers, including cholesterol (821 missing values) and platelet

counts (73 missing values). For continuous variables with missing data, we imputed using the sample mean. For categorical indicators, we used the mode. We also applied alternative approaches with multiple imputation by chained equations (MICE) using CART, as well as model-specific handling of missing values (allowing RF, XGB, and GBMixed with tree base learners to use their default missing-value strategies). In both cases, results were similar or slightly worse than mean/mode imputation, confirming that the chosen approach does not bias our comparative findings.

To evaluate within-patient predictive performance, we implement a temporal train-test split that align with the longitudinal structure. For each patient with multiple visits, we include all but their last observation in the training set, while reserving their final observation for the test set resulting in 1660 training observations and 285 test observations. This approach simulates the real-world scenario of using a patient’s history to predict their future outcomes.

C.2 Evaluation of Models

We assess model performance using four criteria: (i) predictive accuracy measured by mean squared error for held-out data, (ii) estimation of the treatment effect for D-penicillamine versus placebo, (iii) recovery of patient-specific random effects, (iv) prediction interval coverage, and (v) inspection of partial dependence plots to evaluate nonlinear covariate effects identified by GBMixed.

C.3 Linear Mixed-Effects Model

We apply a linear mixed-effects model with a random intercept for each patient.

The random effects structure shows substantial variability in baseline SGOT levels across patients, with an intercept variance of 0.101 (SD = 0.318). The residual variance is estimated at 0.083 (SD = 0.288), indicating that a considerable proportion of the variation is explained by between-patient differences.

Fixed effects estimates are reported in Table 9. We observe a statistically significant treatment effect for D-penicillamine (drug1) of -0.093 ($t = -2.27$), suggesting that treated patients exhibit lower SGOT levels relative to placebo. Age, sex, bilirubin, alkaline phosphatase, edema, months, and disease stage also emerge as strong predictors.

The LMER baseline achieves a test MSE of 0.1631 providing strong accuracy relative to machine learning benchmarks such as random forest (0.157) and XGBoost (0.164), that only include fixed effects. The LMER baseline attained an empirical coverage of 95.4 percent for nominal 90 percent prediction intervals, based on model-based variance component estimates. This over-coverage suggests conservative interval calibration, consistent with the parametric assumptions of the mixed-effects framework.

This random intercept model serves as the reference point for evaluating GBMixed and alternative machine learning approaches. While it provides strong predictive accuracy and clinically interpretable

Table 9: Fixed effect estimates from the linear mixed-effects model with random intercepts for patients. Variable names follow the `pbc` dataset.

Variable	Estimate	Std. Error	t value
(Intercept)	5.257	0.194	27.139
months	-0.0278	0.0039	-7.168
drug (D-penicillamine)	-0.0929	0.0409	-2.270
age (years)	-0.0119	0.0020	-5.875
sex (female)	-0.1561	0.0644	-2.423
ascites	0.0186	0.0376	0.494
hepatomegaly	0.0152	0.0200	0.762
spiders	0.0427	0.0228	1.873
edema (0.5)	-0.0043	0.0276	-0.155
edema (1.0)	0.1144	0.0427	2.681
stage (2)	0.1324	0.0477	2.775
stage (3)	0.1534	0.0481	3.191
stage (4)	0.1451	0.0512	2.837
bili	0.0380	0.0030	12.659
alk.phos	0.000021	0.000008	2.662
chol	0.000061	0.000072	0.857
albumin	-0.0429	0.0232	-1.851
platelet	-0.000046	0.000130	-0.353
protime	0.0060	0.0078	0.771

effects, it is limited by its linear functional form and inability to capture nonlinear interactions from biomarkers.

C.4 GBMixed Linear Mixed-Effects Model

To establish a baseline for comparison, we use GBMixed to approximate an LMER by employing OLS base learners for the mean function and constant updates for the random effects and residual variance components. This configuration ensures that GBMixed mirrors the structure of the linear mixed model, allowing direct assessment of equivalence.

Figure 13 presents the test predictions (combining both fixed and random effects) from LMER and GBMixed. The near 1:1 relationship between the two sets of predictions confirms that GBMixed reproduces the LMER results.

C.5 GBMixed Nonparametric Mixed-Effects Model – MARS

We next apply GBMixed with multivariate adaptive regression splines (MARS) as base learners, allowing the model to capture smooth nonlinear effects and interactions that cannot be represented within a linear framework. This configuration converges after approximately 111 boosting iterations. The random effect estimates remain similar to those from the LMER baseline, with an intercept variance of 0.075. In terms of predictive accuracy, the MARS configuration achieves a test MSE of 0.139, representing a clear improvement over the LMER baseline (0.163).

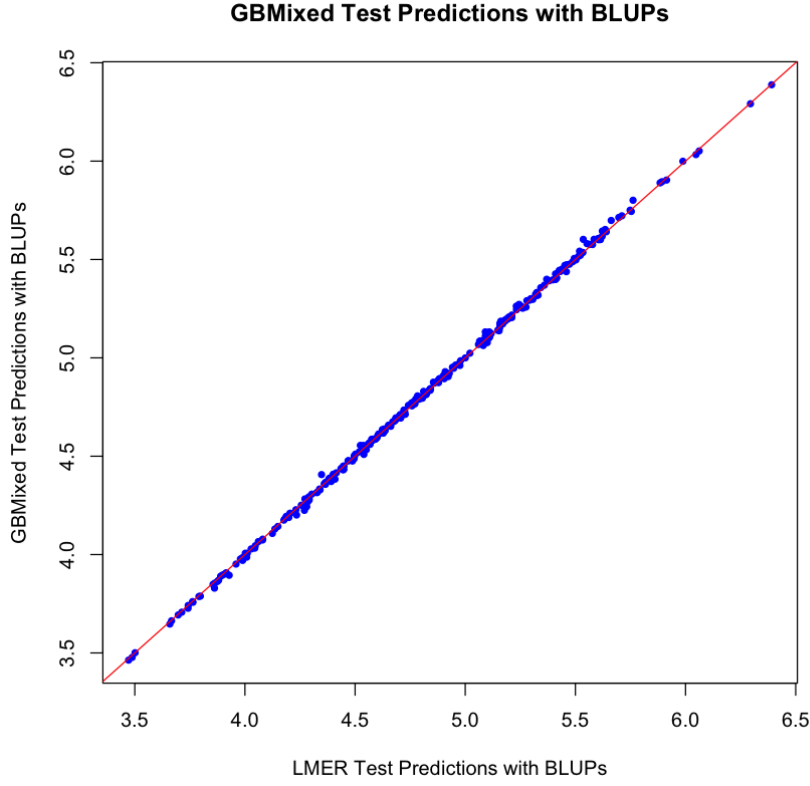


Figure 13: Comparison of test predictions from LMER and GBMixed with OLS base learners.

In addition, the empirical coverage is 92.6 percent for nominal 90 percent prediction intervals, computed using the model’s estimated variance components. This corresponds to a 2.8 percentage point improvement in coverage relative to the linear mixed-effects baseline with homogeneous random effects, indicating more accurate uncertainty calibration under the flexible nonparametric specification.

These results demonstrate the ability of GBMixed to retain the strengths of mixed-effects modeling, particularly its capacity to account for within-patient correlation, while flexibly modeling nonlinear relationships among covariates.

C.6 Summary and Key Insights

This supplementary analysis reinforces the principal findings reported in Section 6.1. Models fitted using GBMixed are also highly interpretable: variable-importance rankings and partial-dependence plots reveal smooth nonlinear relationships and clinically meaningful interactions among biomarkers, particularly for alkaline phosphatase, bilirubin, and albumin. Among all methods compared (Table 5), only GBMixed with MARS base learners achieves the lowest test MSE, while random forest ranks second but shows signs of overfitting (performing well on training data yet worse than LMER within the treatment subgroup).

Appendix D: Supplementary Materials for the PSID Application

D.1 Data Setup

The PSID7682 dataset from the `AER` package contains annual observations for U.S. individuals from 1976 to 1982 (Cornwell and Rupert, 1988). Each of the 595 individuals were observed in all seven years, yielding a balanced panel of 4,165 total observations.

The data are split into a training period (1976–1980) and a test period (1981–1982), yielding 2,975 and 1,190 observations respectively. The panel is balanced across all years and individuals. We model the log of wage as a function of education, experience, occupation, industry, gender, union status, and regional indicators, capturing key determinants of earnings. Experience is one of the key predictors ranging from 0–50 years and is later decomposed into within and between components.

D.2 Evaluation of Models

We assess model performance using four criteria: (i) predictive accuracy measured by mean squared error for held-out data, (ii) recovery of patient-specific random effects, (iii) prediction interval coverage, and (iv) inspection of partial dependence plots to evaluate nonlinear covariate effects identified by `GBMixed`.

D.3 Ordinary Least Squares (Baseline)

As a benchmark, we begin with an ordinary least squares regression model that ignores the longitudinal structure of the data. The model includes all available covariates and all observations are treated as independent.

The test MSE is 0.1933, which provides a baseline for evaluating the gains achieved by clustered data models that explicitly account for subject-level variation.

D.4 Random-Intercept Modeling

D.4.1 Linear Mixed Effects Model

We fit a linear mixed-effects model which includes the same covariates as the OLS baseline but adds a random intercept for each individual (`id`), thereby accounting for repeated measurements within subjects. This specification captures within-individual correlation in wage levels that OLS models cannot.

The estimated variance components indicate substantial heterogeneity across individuals, with a random intercept variance of 0.516 and a residual variance of 0.024. This suggests that between-person differences in baseline wages account for most of unexplained variation in the data.

We evaluate two forms of prediction on the test set: fixed effects only predictions, and BLUPs to capture subject-specific deviations.

Including the random intercepts leads to a substantial improvement in predictive accuracy, with the test MSE dropping from 0.5809 (fixed effects only) to 0.0395 (fixed + random effects). This highlights the importance of accounting for persistent individual differences in this panel data.

D.4.2 Non-Clustered Machine Learning Models

For comparison, we fit two non-clustered ensemble models: a random forest and an XGBoost model. Both models use the same covariates as the linear and mixed-effects models but do not include any grouping or random effects structure.

Optimal hyperparameters were selected through tuning. The random forest achieved a test mean squared error of 0.1386, while the XGBoost model achieved a test MSE of 0.1517.

Although both models outperform the OLS baseline, their accuracy remains below that of the linear mixed-effects model, highlighting the importance of explicitly modeling within-individual correlation in longitudinal earnings data.

D.4.3 GBMixed Linear Mixed-Effects Model

We fit the GBMixed algorithm using an ordinary least squares base learner to replicate the LMER random-intercept model. The same covariates and group structure are used, with 300 boosting iterations and learning rates of 0.03 for both mean and variance components. The model converged after 183 iterations.

Estimated coefficients closely matched the LMER results. The estimated random-effect variance was 0.455 and the residual variance 0.0185, both comparable to the LMER estimates (0.516 and 0.024).

Predictive accuracy was similar as well: the test MSE was 0.5506 using fixed effects only and 0.0405 when including random effects. The GBMixed BLUPs were highly correlated with the LMER-based BLUPs ($R^2 = 0.9997$). These results confirm that GBMixed recovers the standard linear mixed-effects model when fitted with linear base learners and provides a referenced starting point for further nonparametric modeling.

D.4.4 GBMixed Nonparametric Mixed-Effects Model – MARS

We then fit GBMixed using a multivariate adaptive regression splines (MARS) base learner to introduce nonlinear mean structure. The model used 500 iterations with moderate learning rates (0.02) and the same random-intercept structure as previous models. The optimal iteration was reached at 467.

Introducing nonlinear terms substantially changed the model's variance decomposition. The estimated random-effect variance dropped to 0.133, while the residual variance increased to 0.028, indicating that the nonlinear mean model captured much of the within-subject correlation previously modeled

through random effects. This improved the fixed-effects prediction (test MSE = 0.2042) but weakened BLUPs (test MSE = 0.0810).

This trade-off persisted across a wide range of hyperparameter settings and when using tree-based base learners.

D.5 Detecting Heterogeneity with GBoost

To test the assumption of homogeneous random effects, we apply the GBoost variant of GBMixed, which models the random-effect variance as a function of group-level covariates while maintaining linear fixed effects. The first model includes all observation-level covariates (as group-level summaries) as potential predictors of group-level variance, allowing us to identify which factors drive heterogeneity in random effects.

Variable importance analysis from the random-effects variance model is reported in Table 10. Experience dominates as the key driver of heterogeneity, contributing nearly half of the total importance.

Table 10: Variable importance in the random-effect variance model (GBoost).

Variable	Importance
EXP	0.478
WKS	0.155
ED	0.072
SMSA	0.072
MS	0.069
UNION	0.066
IND	0.044
OCC	0.033
SOUTH	0.013

Given this result, we re-estimate the model using only Experience as a group-level covariate in the random-effects variance model. This yields an optimal iteration of 924. The estimated average random-effect variance is 0.496, and the residual variance is 0.017, both more consistent with prior results for LMER but now reflecting heterogeneity across experience levels.

The partial dependence plot for Experience (Figure 9) in the random-effect variance model exhibits a clear U-shaped pattern: relatively stable variance for low experience (1–7 years), a decline near mid-career (around 16 years), and a steady increase thereafter (up to 35 years). This pattern indicates that within-subject correlation in wages is weakest for mid-career individuals, with much stronger correlation observed for early- and late-career workers. In other words, wage trajectories are most stable across time within individuals at the beginning and end of their careers, while mid-career workers show more independent year-to-year variation likely from career changes or progression.

The test MSE for fixed effects alone is 0.9413, while including random effects reduces it to 0.0347 showing that predictive accuracy improves when random-effect heterogeneity is incorporated, albeit with a smaller relative contribution from fixed effects. These results confirm that GBoost captures

covariate-dependent variation in random-effects, providing a flexible extension of the standard mixed-effects framework.

D.6 Modeling Heterogeneity

The GBoost variant of GBMixed improves predictive accuracy in the PSID data but raises the question of why random intercepts are heterogeneous across individuals and whether a richer structure can better explain this effect. To investigate, we plot wage trajectories for a random subset of subjects by experience. This provides a visual diagnostic of between-subject and within-subject variability, revealing whether differences arise mainly from baseline wage levels (intercepts), wage growth rates (slopes), or both.

The trajectories in Figure 10 reveal clear evidence of heterogeneity across individuals. First, the spread of starting points indicates substantial variation in baseline wage levels, supporting the inclusion of random intercepts. Second, the slopes differ markedly across subjects, suggesting that random slopes in experience may also be warranted. Third, subjects with more than 30 years of experience exhibit flatter and more stable wage paths, implying reduced within-subject variability late in the career cycle. These features point to distinct between- and within-subject effects of experience that cannot be fully captured by a single covariate.

To capture these patterns, we decompose experience into two orthogonal components: between-subject and within-subject variation. The between-subject component (`EXP_between`) represents each worker's mean experience across all observations, capturing long-term career differences among individuals. The within-subject component (`EXP_within`) is defined as the deviation of experience from the individual's mean, reflecting the short-term change or panel-year effect. This decomposition separates stable cross-subject differences from time-based trends, allowing the model to identify how overall career experience influences wage levels while isolating how incremental experience gained during the panel study affects wage growth.

Under this specification, we refit the linear mixed-effects model by replacing the raw `EXP` variable with its orthogonal components, `EXP_between` and `EXP_within`, and adding a random slope on the within-subject term. The results in Table 6 show a substantial improvement in model fit: AIC and BIC decrease by over 1000 points relative to the untransformed models, while the test MSE with BLUPs improves from 0.0395 to 0.0325.

When the same decomposition is applied to ensemble learners, both random forest and XGBoost exhibit marked gains in predictive accuracy, reducing their test MSE from approximately 0.15 to 0.07. However, these remain less accurate than the mixed-effects models, highlighting the value of explicitly modeling random effects.

Finally, to assess whether additional nonlinear effects remain, we fit GBMixed with a MARS base learner for the mean function. The results show that key predictors such as `EXP_within` and `ED` are

largely linear, with only mild curvature in `WKS` and `EXP_between`, producing a small further reduction in test MSE to 0.0321.

D.9 Summary and Key Insights

GBMixed reproduced and extended the linear mixed-effects structure observed in the PSID data. Using an OLS base learner, it closely matched the LMER estimates. With MARS, nonlinear mean effects reduced within-subject correlation by absorbing shared variance. Under GBoost, random-effect variance was found to depend strongly on experience, revealing a clear U-shaped pattern in within-subject correlation across career stages.

Driven by the GBoost insight, introducing the experience decomposition provided a key interpretive and predictive improvement. By separating `EXP` into orthogonal between- and within-subject components, the models could distinguish long-term career differences from short-term panel effects. When combined with a random slope on the within-subject term, this specification delivered a much better and simpler representation of individual wage dynamics, achieving a step change in performance.

Adding nonlinear base learners produced only marginal further gains, confirming that the main structure of heterogeneity was captured by the decomposed experience terms and their random slopes. Overall, these results demonstrate that GBMixed can flexibly model nonlinear and heterogeneous variance structures in longitudinal data, providing predictive accuracy and interpretability for optimal model construction.

Appendix E: Draft Package Implementation and Runtime

The methodology is implemented in an `R` package, which provides core fitting functions for `gbmixed` and its extensions (RBoost, GBoost, GRBoost). The package supports multiple choices of base learners, flexible specification of random effects, prediction functions, and diagnostic plotting functions.

Runtime results are reported in minutes, based on experiments run on a GCP server with 32 cores and 6 parallel workers. Random forest (`ranger`), gradient boosting machines (`xgboost`) and causal forest (`grf`) were each limited to 4 threads. Reported values reflect the accumulated CPU runtime across all threads, providing a fair comparison of computational demands across methods.

Table 11: Runtime (minutes) by Experiment and Method

Experiment	OLS	LMER	RF	XGB	CF	GBMixed
Exp A	0.20	3.45	20.50	15.79	6.36	4.78
Exp B	0.01	0.23	3.82	1.56	8.48	9.89
Exp C	0.01	0.22	4.09	13.59	8.07	10.25

The runtime comparison highlights that OLS and LMER are consistently the fastest due to their

parametric structure, while the machine learning approaches incur higher computational costs. Among these, `gbmixed` is slower in some experiments but comparable or faster in others, with performance influenced by parameter settings and early stopping. Overall, the results suggest a promising baseline for further optimization and parallelization on larger datasets.